

X-Ray Microscopy

Dan COJOC



cojoc@iom.cnr.it

Consiglio Nazionale delle Ricerche
Istituto Officina dei Materiali - Materials Foundry

www.iom.cnr.it

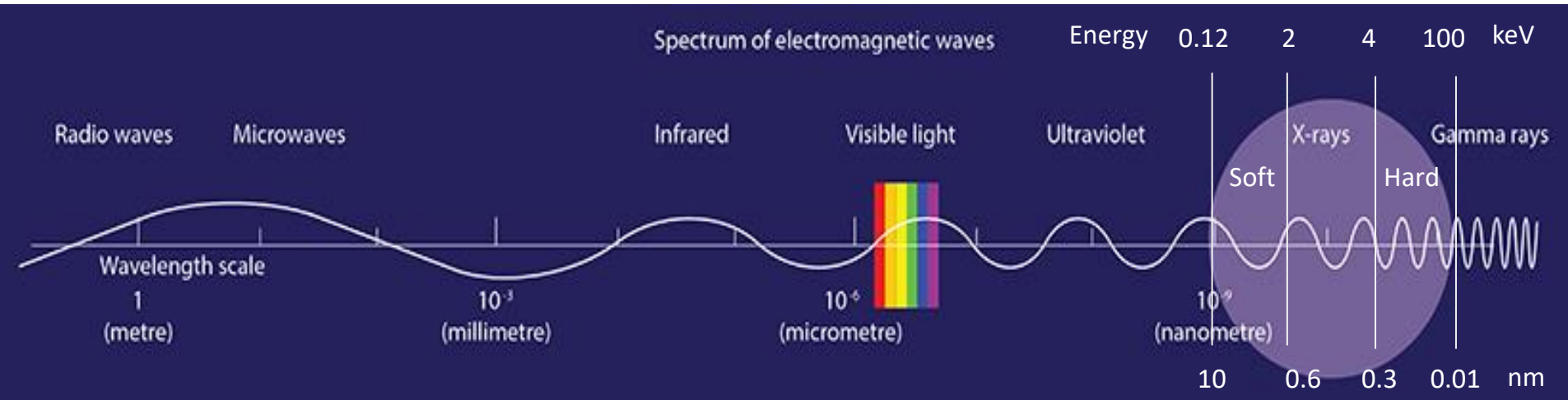
University of Trieste, 2022

Outline

1. ~~Why Atomic Force Microscopy ?~~ WHY X-RAY MICROSCOPY ?
2. How is the image formed in X-ray microscopy ?
3. X-ray microscope components and techniques
4. Radiation damage
5. X-ray microscopy with Synchrotron light
6. Imaging cell morphology and physiology using X-rays (review to read)
7. X-ray diffraction imaging and Free Electron Laser (FEL)

Why X-Ray microscopy ?

X-ray microscopy uses X-ray beam to illuminate samples and produce magnified images.



$$\lambda \text{ [nm]} = 1.24 / E \text{ [keV]}$$

- X-rays penetrate matter far easier than visible light → X-ray microscopy can image the inside of samples opaque for optical (OM) or electron (EM) microscopies.
- X-ray wavelengths (0.03 – 10 nm) are much shorter than visible light (300-800 nm) → XrayM spatial resolution (20 nm) better than OM (200 nm).
- XrayM resolution is lower than SEM (2 nm) and TEM (0.2 nm) but XrayM can operate at atmospheric pressure, with wet samples and can image thicker samples.
- X-ray 3D and 4D (space + time) imaging
- Coherent diffraction imaging with FEL (Free Electron Laser)

X-ray - Historical notes:

- 1895 - Röntgen discovered X-rays
- 1940 - Bragg produced the first usable X-ray image
- 1972 – first use of synchrotron for X-ray microscopy

Contrast mechanisms

As for all microscopies, to get a useful image one needs a good contrast mechanism (CoMe).

The **attenuation of X-rays** when passing through matter:

is the most used CoMe

$$I = I_0 e^{-\mu z} \quad \mu - \text{attenuation coefficient}$$

which is caused by both **absorption** and scattering *: $\mu = \tau_a + \sigma$

X-ray absorption is mainly due to the ionization of atoms → **absorption cross-section**, τ_a depends on the excitation energy of atoms and thus on the **atomic number Z**

For X-ray radiation at a fixed energy (and wavelength) :

$$\tau_a \sim Z^4$$

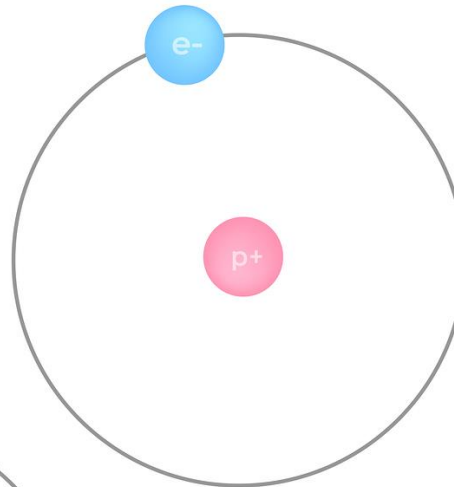
(this is a close approximation for pure metals)

* For X-ray at photon energy $E = 0.31$ keV ($\lambda = 4$ nm), absorption is dominant to scattering in pure metals

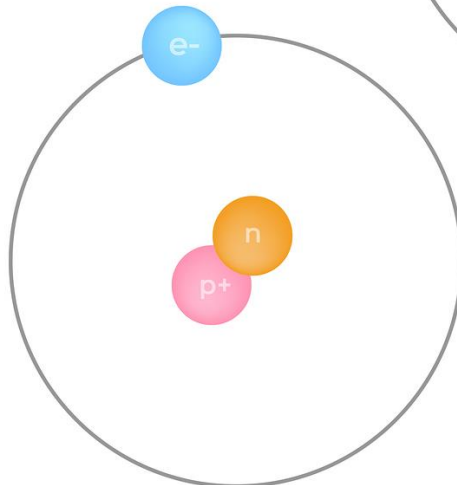
Hydrogen Isotopes

1 Da $\sim 1.66 \times 10^{-27}$ kg

Atomic number $Z=1$
Atomic mass ~ 1 Da

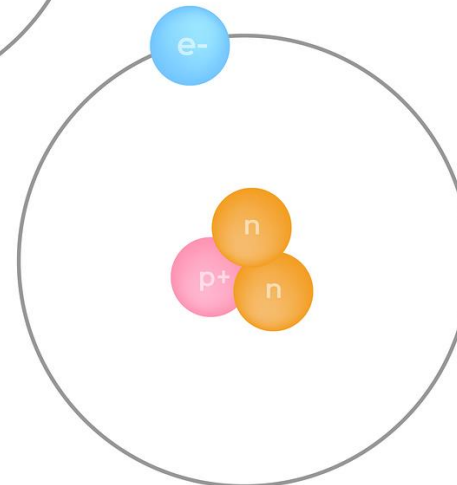


Protium



Deuterium

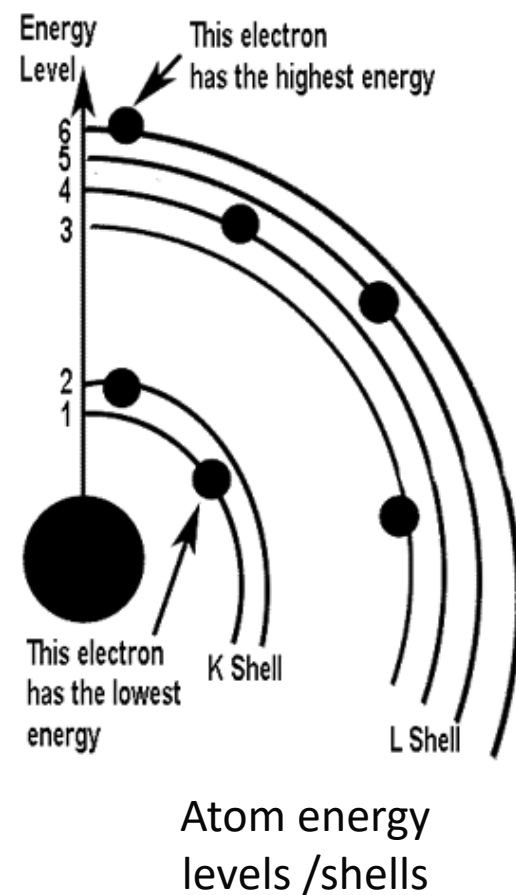
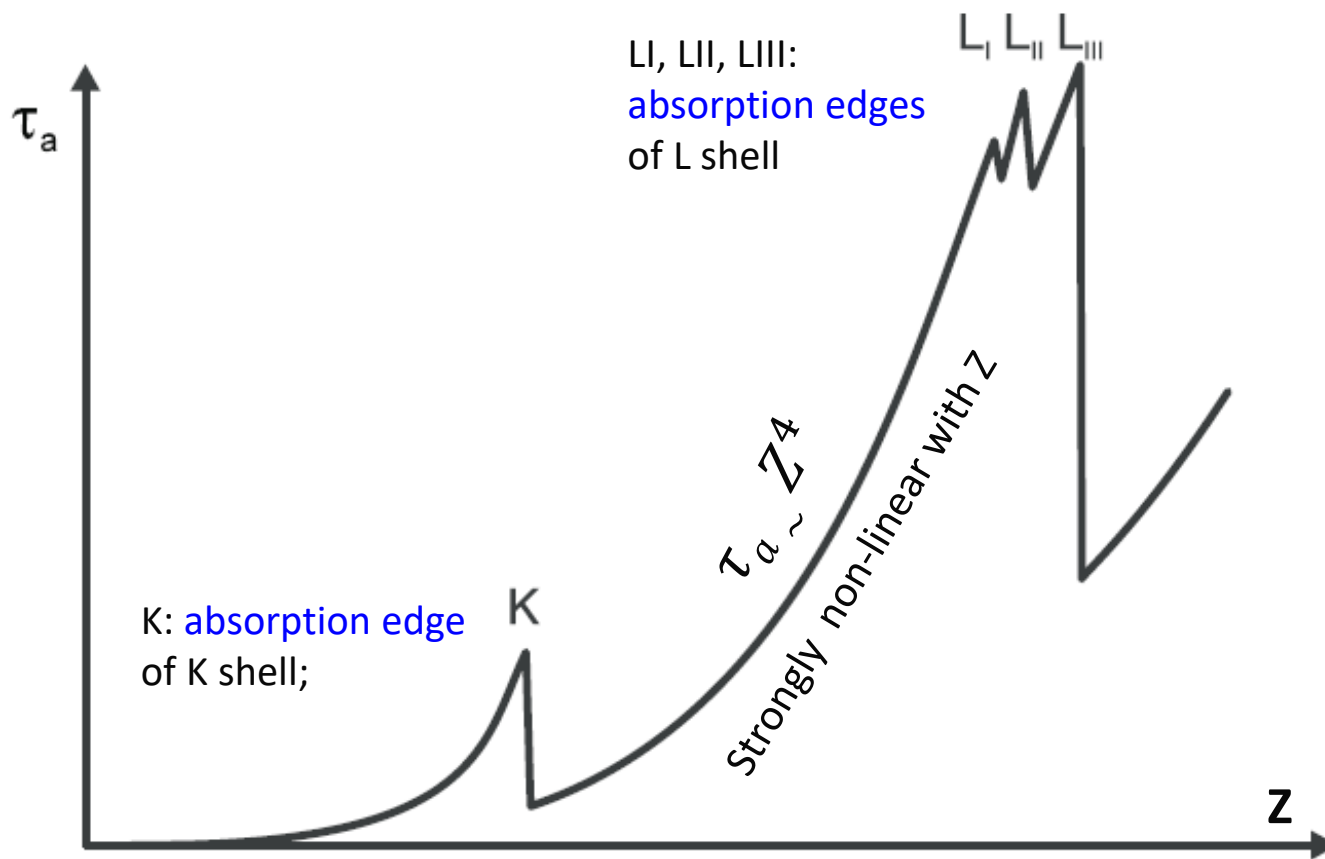
Atomic number $Z=1$
Atomic mass ~ 2 Da



Tritium

Atomic number $Z=1$
Atomic mass ~ 3 Da

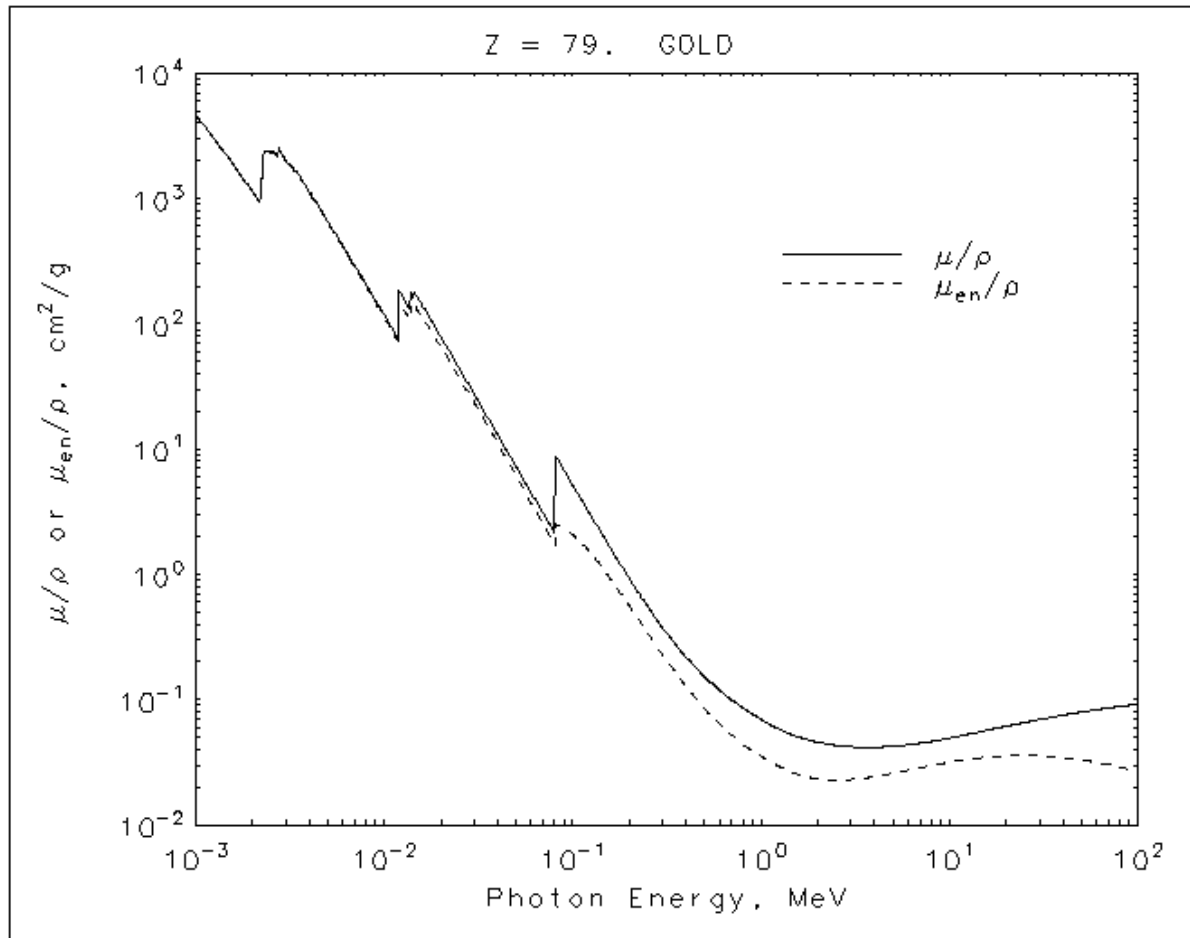
Example (schematic) showing the tendency of the Absorption cross-section coefficient τ_a as a function of the atomic number Z at a fixed x-ray wavelength



presence of “absorption edges” results from increased attenuation of x-rays by photoelectric absorption event at energies equal to binding energies of electrons in the specific element.

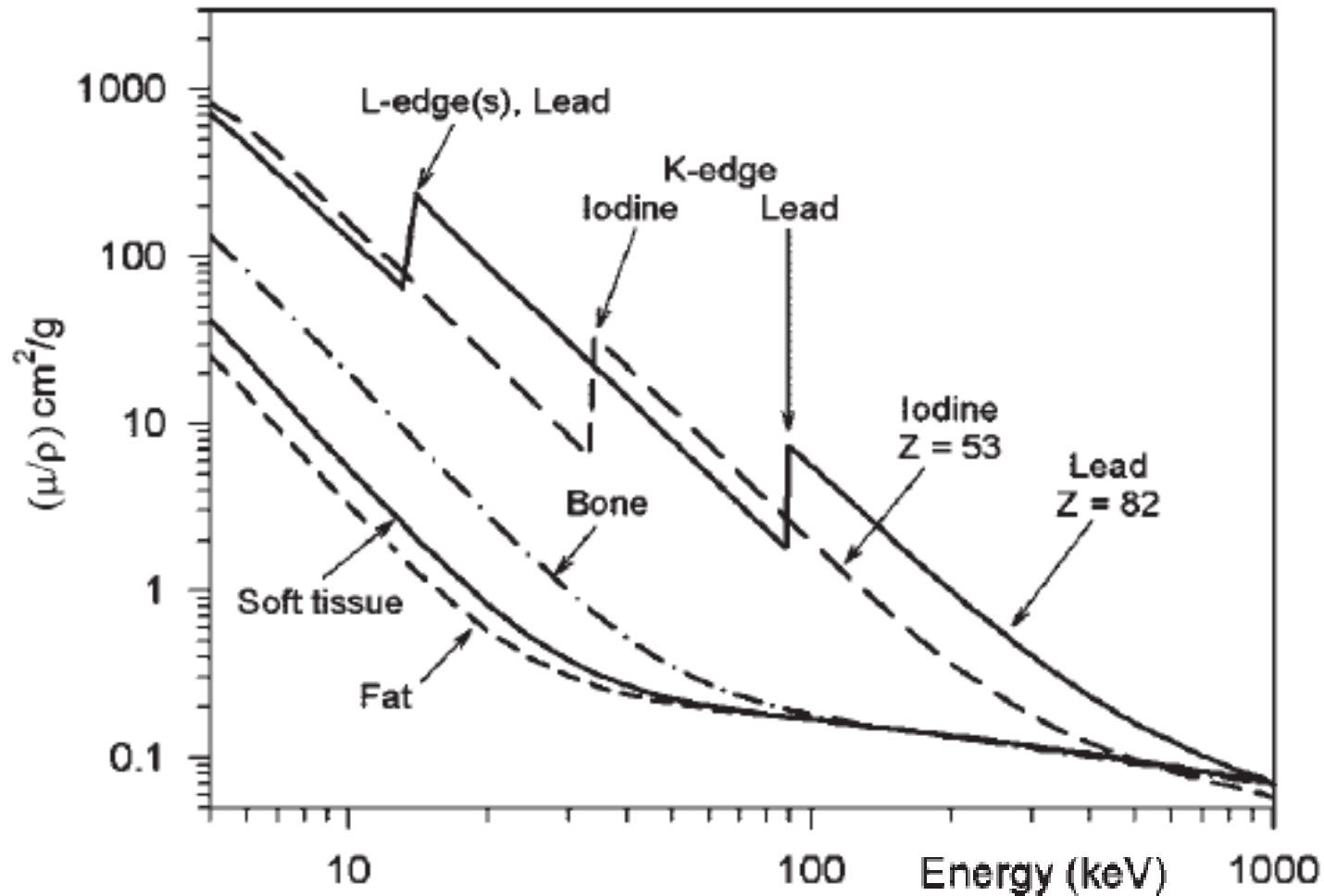
X-ray attenuation coefficient depends on energy of the incident X-ray

Values of the mass attenuation coefficient, μ/ρ as a function of photon energy, for Au



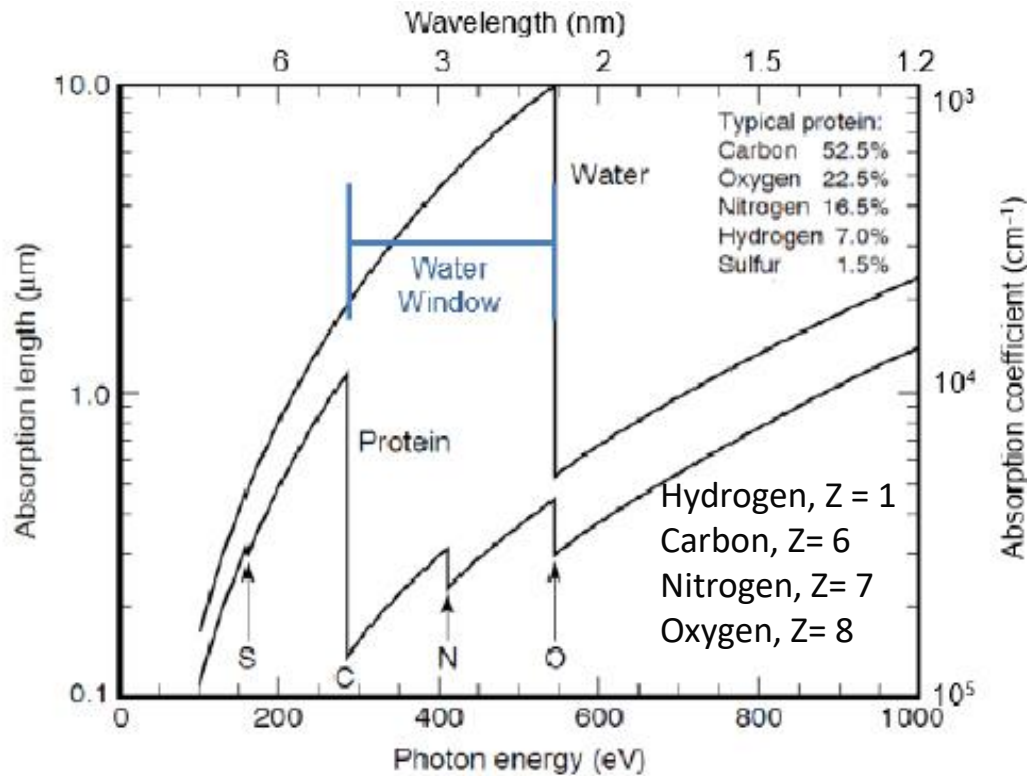
The mass energy transfer coefficient μ_{en}/ρ is the product of the mass attenuation coefficient μ/ρ by the fraction of energy transferred to the charged particles as kinetic energy, by the interacting incident photons.

Mass attenuation coefficient as a function of energy for soft X-ray for several materials encountered in diagnostic x-ray



Mass attenuation decreases at a rate of approximately $1/E^3$ and increases as a function of atomic number Z of the attenuating material at a rate $\sim Z^3$ rather than Z^4 .

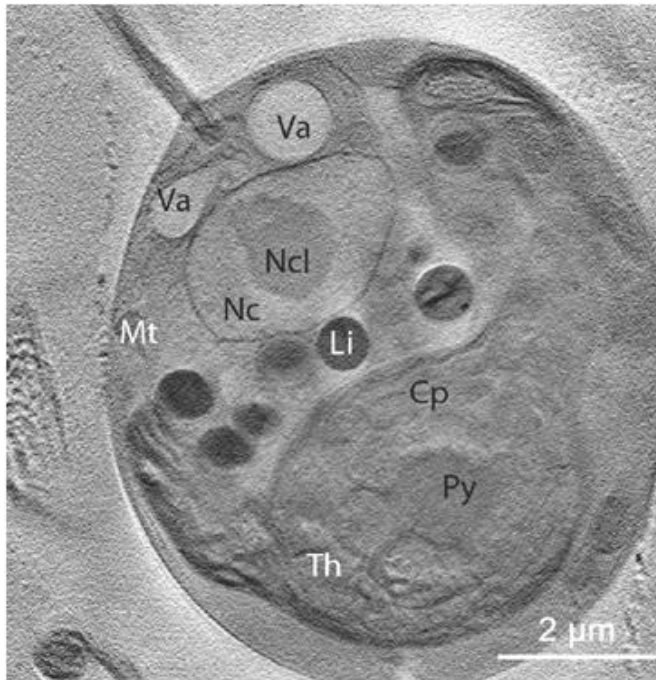
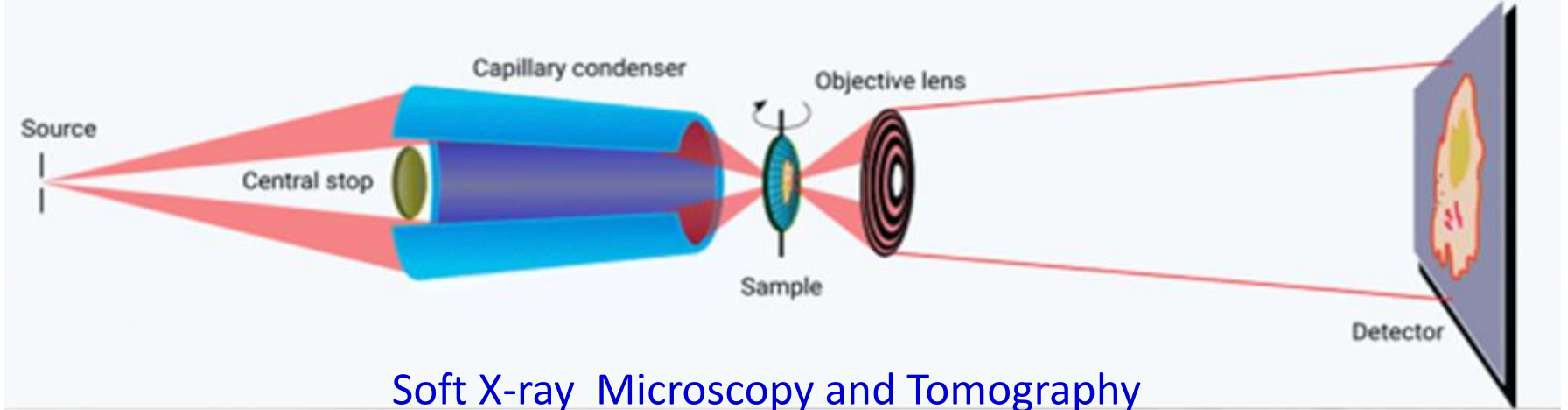
The water window



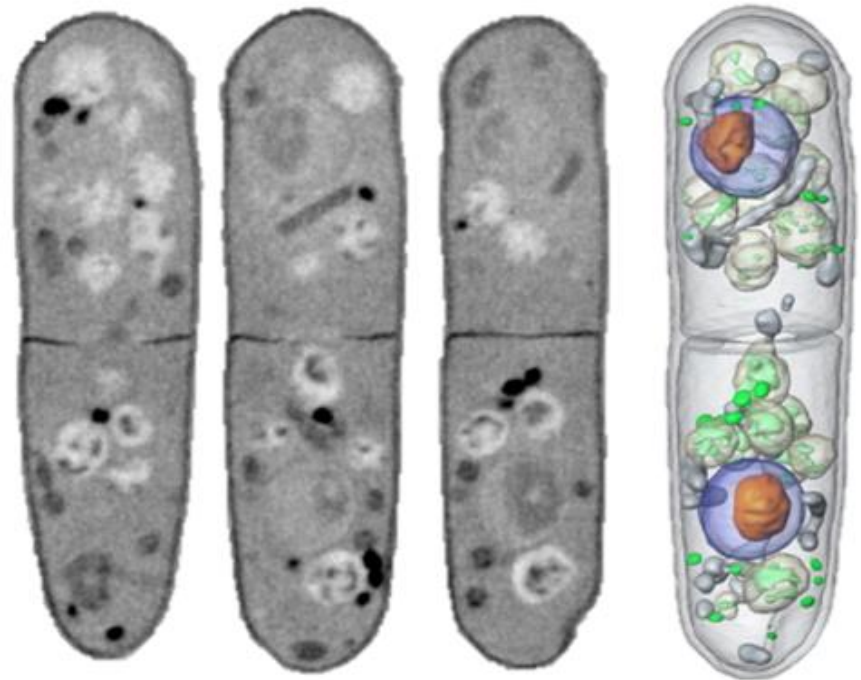
Region of the EM spectrum in which water is transparent to **soft x-rays**. The window extends from K-absorption edge of **carbon** at 282 eV to K-edge of **oxygen** at 533 eV. Water is transparent but carbon (and thus, organic molecules) is absorbing.

→ these photon energies could be used in an x-ray microscope for viewing living specimens

Soft x-ray imaging is carried out at a wavelength in the so-called 'water window' region of the electromagnetic spectrum. This window extends from the K-absorption edge of carbon (4.4 nm wavelength) to the K-edge of Oxygen (2.33 nm wavelength). In this wavelength window, water is transparent to soft x-rays but the carbon-based organic molecules are absorbing. This results in soft x-ray images with a high natural contrast.



SXT tomography slice of *Chlamydomonas*. Chloroplast (Cp); Pyrenoid (Py); Thylakoids (Th); Nucleus (Nc) Nucleolus (Ncl); Vacuoles (Va); Mitochondrion (Mt); Lipid bodies (Li). Bar = 2 μm .



SXT tomography slice of a bacterial sample showing three slices taken from different angles, and reconstructed into a 3D image (right)

Phase contrast mechanism

Starting from the solution of the wave equation describing light propagating in materials

$$E(z,t) = E_0 \exp\left[i\left(\omega t - \left(n_{\text{real}} + in_{\text{imag}}\right)\omega z/c\right)\right] = E_0 \exp\left[i\left(\omega t - \underbrace{n_{\text{real}}\omega z/c}\right)\right] \exp\left(\underbrace{-n_{\text{imag}}\omega z/c}\right)$$

Phase
change Absorption /
attenuation

This equation states that light in a medium of refractive index n oscillates at frequency ω , but experiences a change in its velocity to $v=c/n$.

$n = n_{\text{real}} + j n_{\text{imag}}$

Refractive index (complex value) is a material characteristic

$$I = I_0 e^{-\mu z}$$

Absorption /
attenuation

$$I = |E|^2 \quad \text{with} \quad \mu = 2 n_{\text{imag}}\omega/c$$

Remember ?

How is the complex refractive index defined ?

Refractive index dispersion : $n = n(\omega)$

Refractive index n describes how matter affects the **light** speed

c – the speed of light in vacuum $c = 1/(\sqrt{\mu_0 \epsilon_0})$

v - the speed of light in material $v = 1/(\sqrt{\mu \epsilon})$

$$n = \frac{c}{v}$$

Let us consider the interaction light matter a bit more in detail

The refractive index n is a function of electrical susceptibility χ :

$$n^2 = 1 + \chi$$

The electric susceptibility χ measures the ability of a material to become transiently polarized:

$P \sim \chi E$ P - Polarization E - Intensity of the electrical field

$$\chi = \frac{Nq_e^2}{\epsilon_0 m_e} \left(\frac{1}{\omega_0^2 - \omega^2 + 2i\gamma\omega} \right)$$

Light-matter interaction considering N electrons bound to N atomic nuclei per volume \rightarrow damped harmonic oscillator

γ - the damping coefficient – defined by the inverse of the lifetime of the oscillator

ω_0 – resonance frequency of the oscillator

χ is a complex quantity – EM irradiation induces two independent responses in the material:

dispersion frequency dependent propagation of the beam through the material

absorption frequency dependent energy transfer to the interior structure of the material

\rightarrow n is a complex quantity:

$$n = n_{real} + j n_{imag}$$

$$n = n_{real} + j n_{imag}$$

Complex refractive index $n = n(\omega)$

Normal dispersion

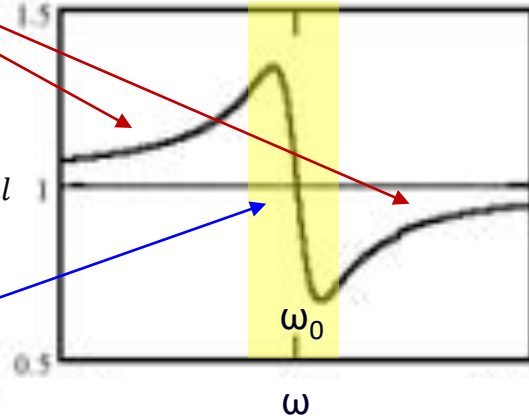
$$\frac{dn}{d\omega} > 0$$

n_{real}

Anomalous dispersion

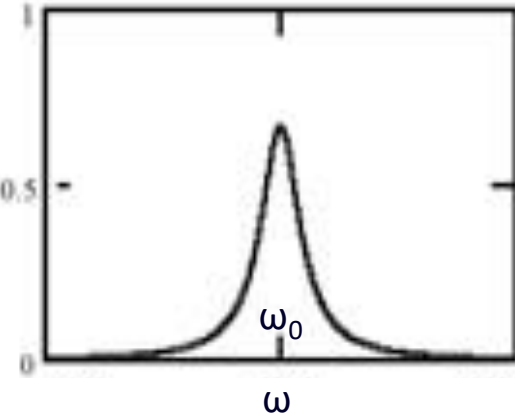
$$\frac{dn}{d\omega} < 0$$

Dispersion



Absorption

n_{imag}

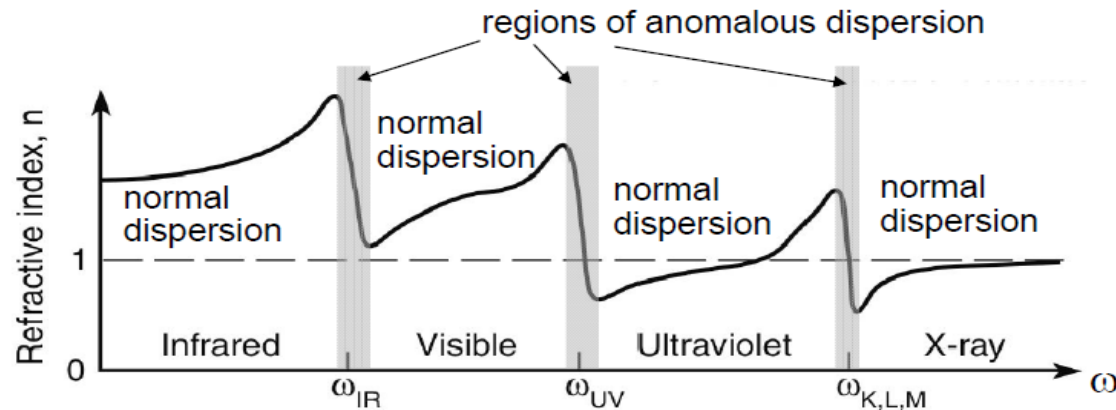


Dispersion and Absorption of EM radiation by dielectric

- The real part of the refractive index, n_{real} , is what we normally call the refractive index in Optics.
- Tabulated values of the refractive index (often measured at 589 nm) refer to n_{real} .
- Far from resonance, n_{real} slightly increases with ω . Near the resonance frequency ω_0 , n_{real} oscillates with $\omega \rightarrow$ **anomalous dispersion**, then it again increases with ω .
- The imaginary part of the refractive index, n_{imag} is very weakly dependent of ω . Near the resonance, n_{imag} increases sharply to a maximum, then falls as $\omega > \omega_0$

Refractive index as a function of frequency $n = n(\omega)$ along the EM spectrum

Since resonance frequencies exist in many spectral ranges, the refractive index varies in a complicated manner.



This illustrates a typical distribution of resonances, with electronic resonances in the UV; vibrational and rotational resonances in the IR, and core electronic resonances occur in the x-ray region.

n increases with frequency, except in "anomalous dispersion" regions. But the overall trend is a decrease in n , as ω increases.

For all chemical materials $n > 1$ at all EM frequencies
but a region of UV X-rays for which $n < 1$!!!

Q: does this mean the speed of X-rays can be higher than the speed of light in vacuum ?

Look at the middle-left figure below, where the phase velocity is greater than the group velocity. The red dot indicates the phase velocity, moving along with the peak of a wave. But the signal or pulse (i.e. the information) is represented by the broad peak enveloping the group of waves. It travels more slowly than the phase velocity, and the blue dot indicates how fast this travels as it moves along with the signal pulse.

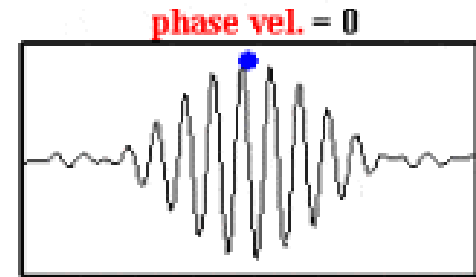
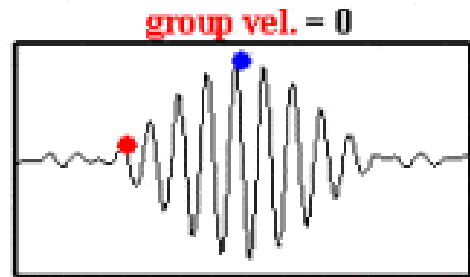
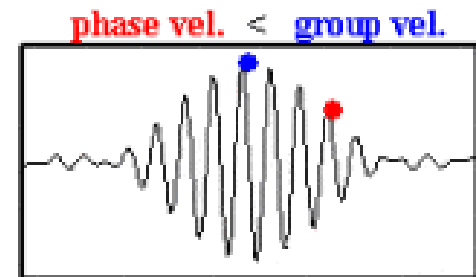
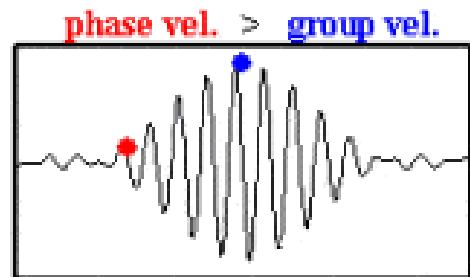
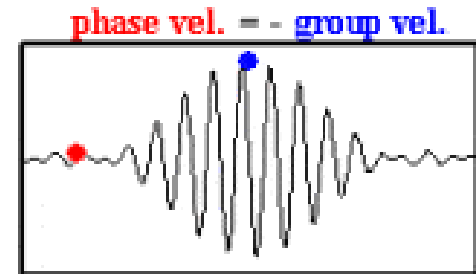
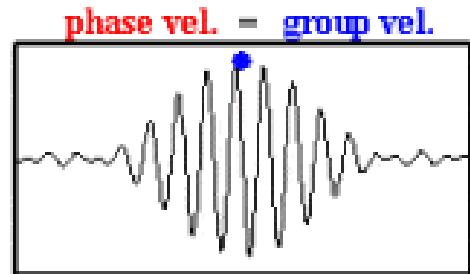
Phase velocity

$$v_p = \frac{\omega}{k}$$

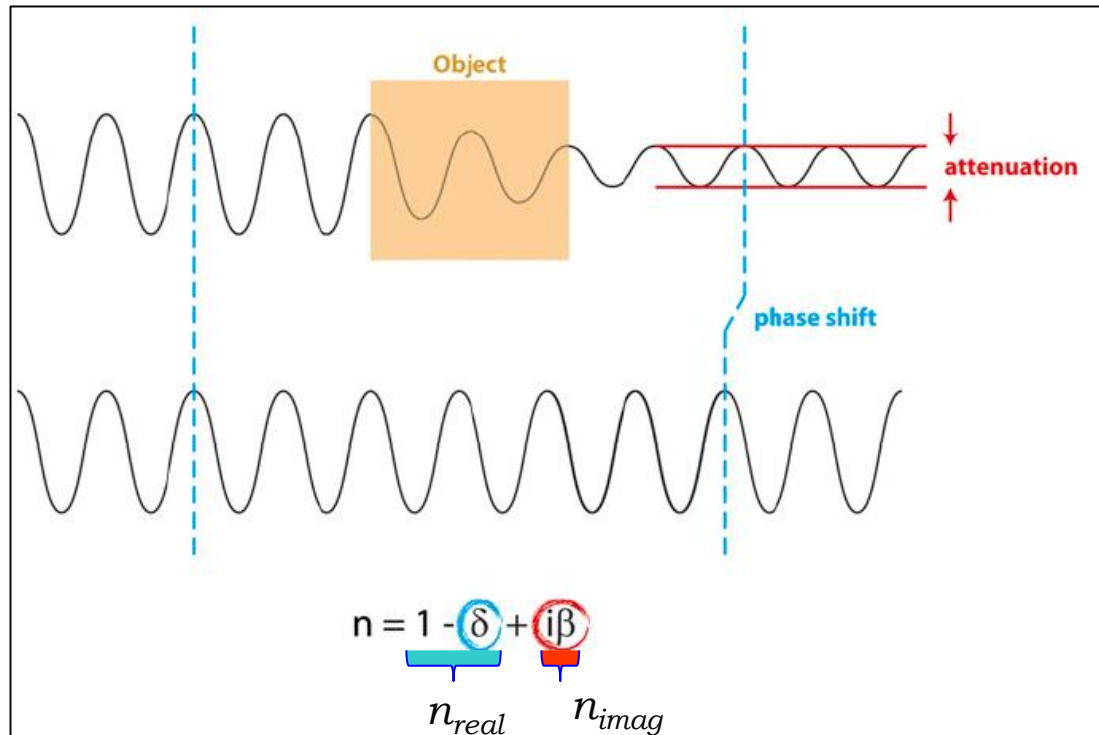


Group velocity

$$v_g = \frac{\Delta\omega}{\Delta k}$$



Contrast mechanisms (summary): attenuation and phase



The differences in **attenuation**, and thus image contrast, depend on tissue density: the denser a certain type of tissue, the less radiation will penetrate.

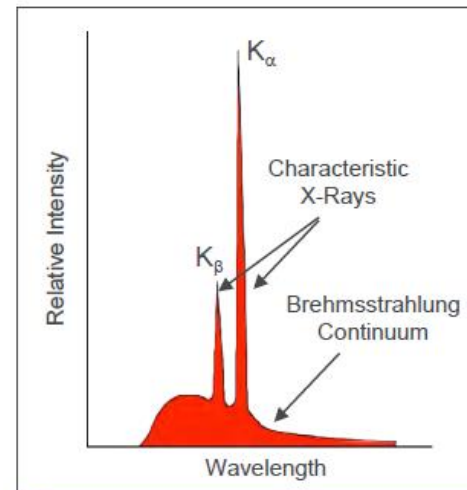
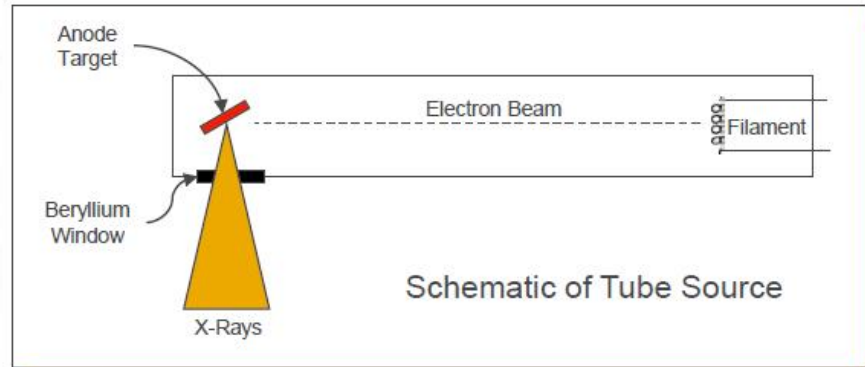
Additionally, the X-ray wave penetrating a medium with refractive index n gets **phase shifted** relative to the original X-ray wave. This phase shift is detected in phase-contrast imaging.

For biological tissues and the X-ray energies typically used in medical imaging, $\delta \gg \beta$,

→ **phase imaging becomes important.**

Example: @10 keV ($\lambda = 0.12$ nm), a model biological specimen of empirical formula $H_{50}C_{30}N_9O_{10}S$ and thus mass density $\rho = 1.35$ g/cm³ exhibits values of $\delta = 3 \times 10^{-6}$ and $\beta = 6.8 \times 10^{-9}$

X- ray tube source



X- ray tube characteristics

- Brightness max 10^8 ph/(s mrad DE/E mm²)
- Beam size (diam) – 1 mm to 10 μ m (focused)
- Characteristic lines broader than 0.5 eV
- Poor focusing, no tunability – no spectroscopy

Other lab sources: X-Ray laser plasma

Problem:

Which is the minimum wavelength gained from electron accelerated by an electric field $V=50$ kV?

The maximum efficiency that can be obtained is when all the kinetic energy of the electron is converted into the energy of the photon:

Kinetic energy = photon energy $eV=hf$ or $eV = \frac{hc}{\lambda}$

- $eV= 50 \times 10^3 \times 1.6 \times 10^{-19} \text{ [kV} \times \text{C]} = 8 \times 10^{-14} \text{ J}$
- $h = 6.6 \times 10^{-34} \text{ Jsec}$
- $c = 3 \times 10^8 \text{ m/sec}$
- $hc = 1.98 \times 10^{-24} \text{ Jm}$
- $\lambda = hc/eV = 1.98 \times 10^{-24} \text{ Jm} / 8 \times 10^{-14} \text{ J} = 0.25 \times 10^{-10} \text{ m} = 0.025 \text{ nm}$

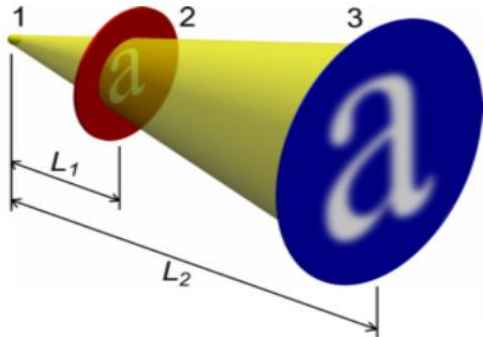
Remember $\lambda(\text{nm}) = 1.24 / E(\text{keV})$

In effetti e la dimostrazione

X-ray microscopes – components and characteristics

X-ray full field with shadow projection microscope

Lens free



Magnification

$$M = \frac{L_2}{L_1}$$

Resolution

$$\sim D_{Source}$$

With lens (Fresnel zone plate)

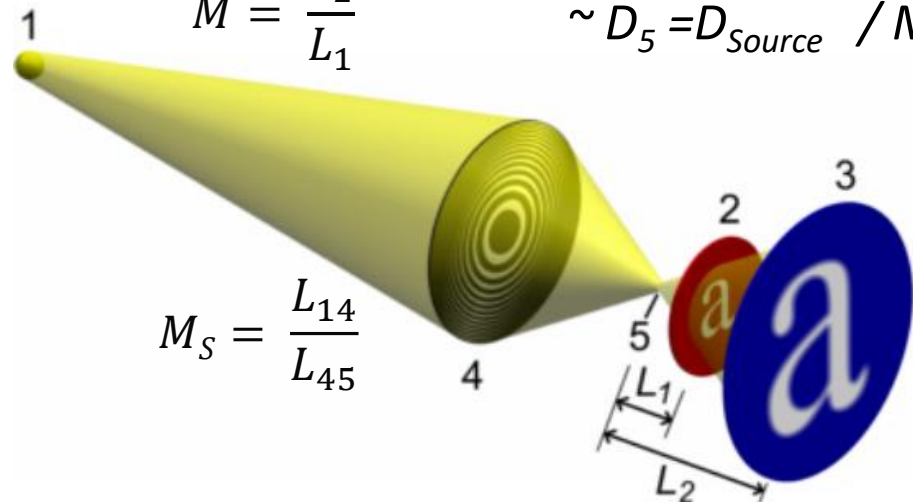
For better resolution

Magnification

$$M = \frac{L_2}{L_1}$$

Resolution

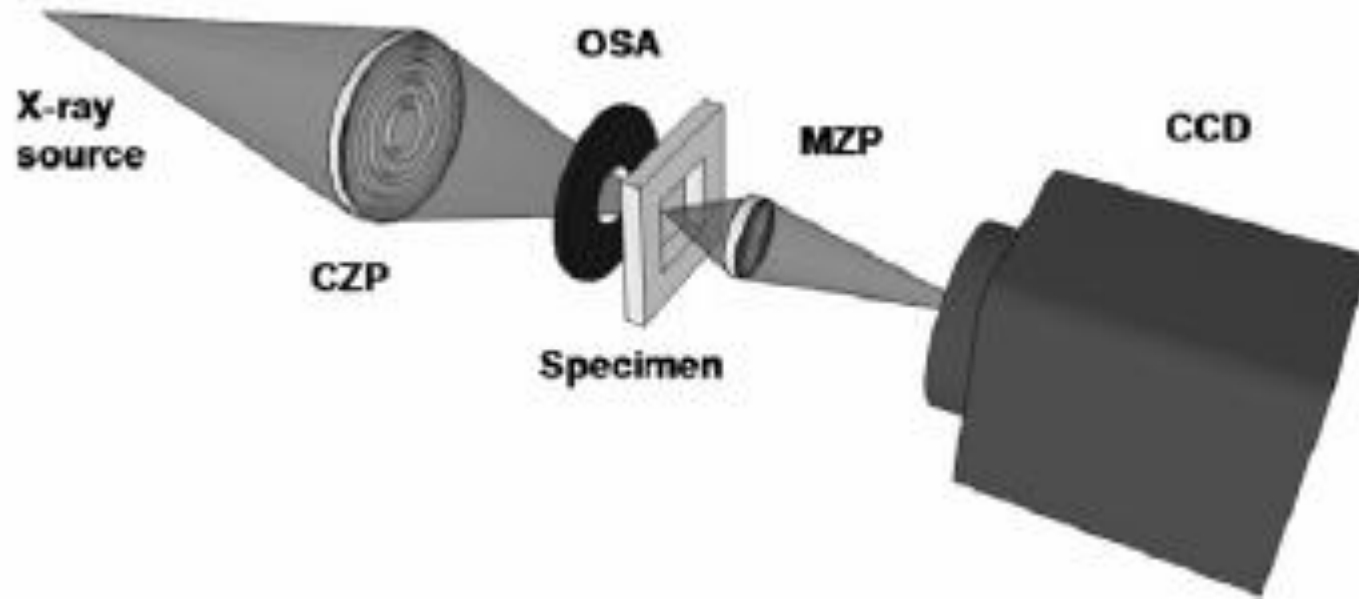
$$\sim D_5 = D_{Source} / M_S$$



- 1 - Source
- 2 - Sample
- 3 - Image
- 4 – Zone Plate (why zone plate ?)
- 5 – Demagnified image of the source

$$M_S = \frac{L_{14}}{L_{45}}$$

Full field transmission X-ray microscope (TXM) with imaging lens (FZP)

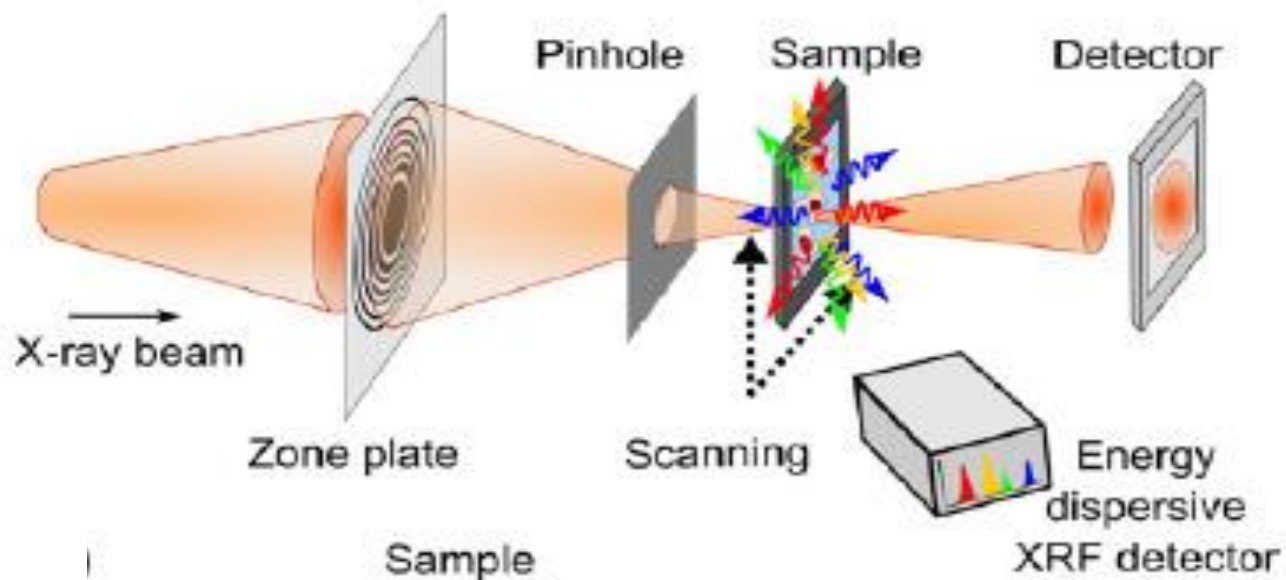


Optical scheme of a full-field imaging microscope (TXM) with x-ray source, condenser zone plate (CZP), specimen, the micro zone plate (MZP) functioning as an objective lens, and a charge-coupled device camera (CCD).

OSA = Optical Sorting Aperture (why ?)

Phase contrast PC imaging : Zernike PC is similar with that in OM, DIC is obtained by using a special FZP as objective (which generate two spot PSF -Point Spread Function

Scanning transmission X-ray microscope (STXM)



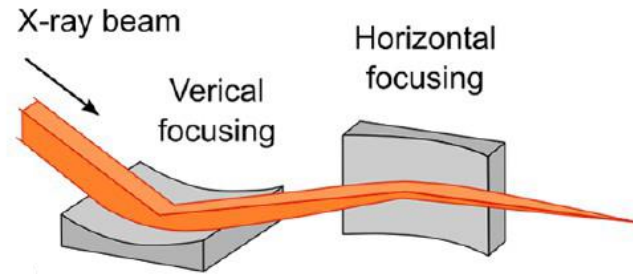
(STXM) with an X-ray fluorescence (XRF) detector

X-ray microscopy – optical components

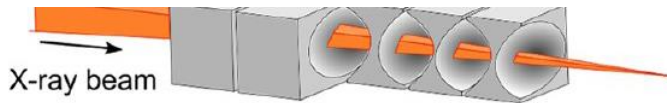
● Diffractive Condenser
for sample illumination



Reflective Focusing Mirrors

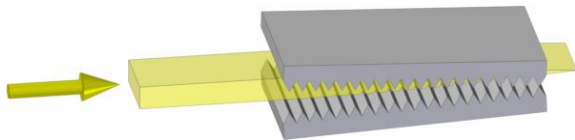


Refractive focusing X-ray lens made of
a row of holes in a metal bar
(Beryllium)

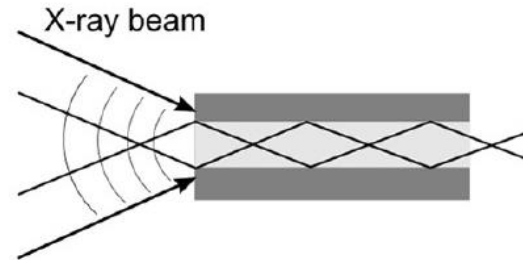


Because $n_{\text{real}} < 1$!

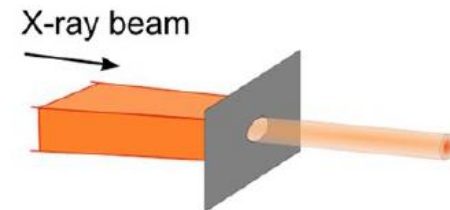
Alligator lens with line focus



Focusing wave guides (capillaries)

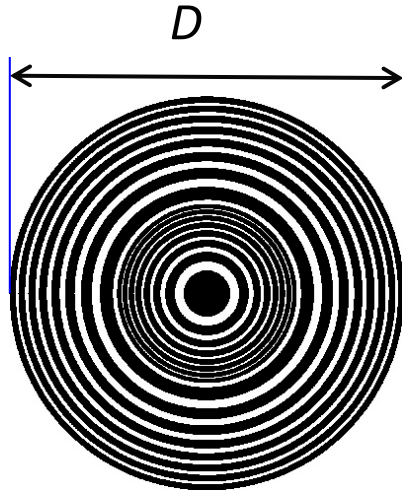


Pinhole



Focusing and Imaging Zone Plate

A ZP is a diffractive element composed by multiple concentric zones of which width gets thinner to the outer zone.



FZP equation

$$r_n^2 = n\lambda f + n^2 \lambda^2 / 4$$

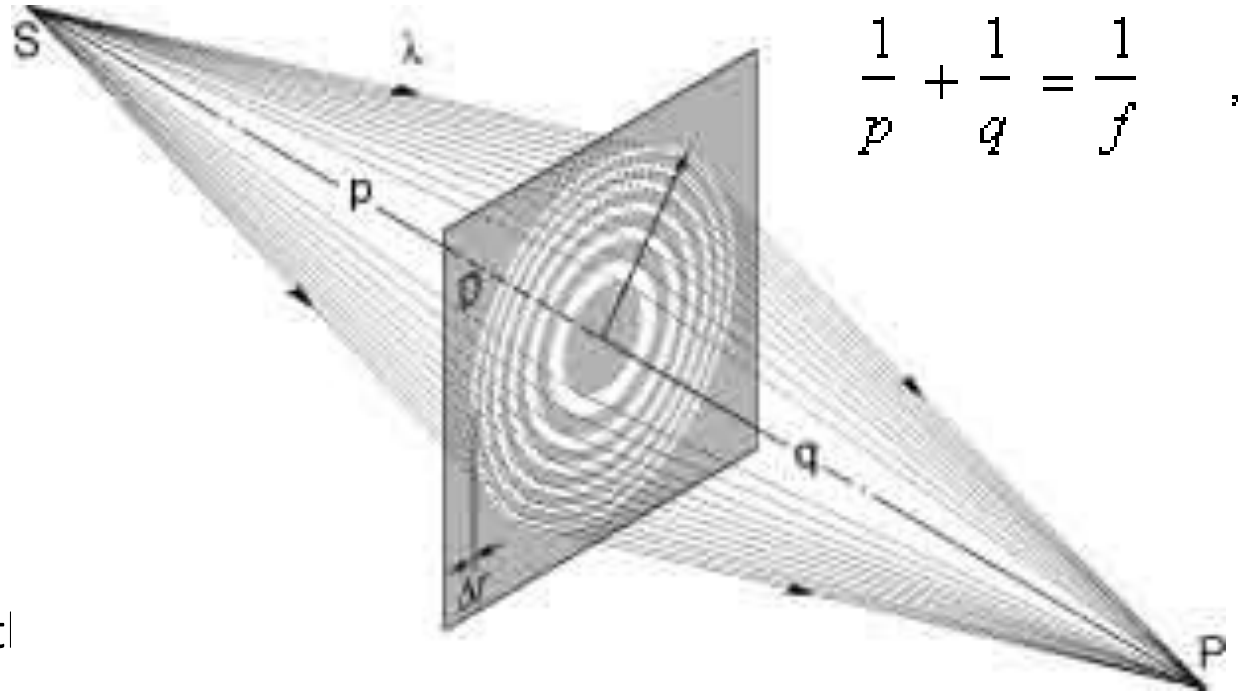
f – first order focal length

r_n – radius of n -th zone

λ – wavelength

$\Delta r = r_n - r_{n-1}$ the outer zone width

$$\Delta r = D/4N$$



$$\frac{1}{p} + \frac{1}{q} = \frac{1}{f}$$

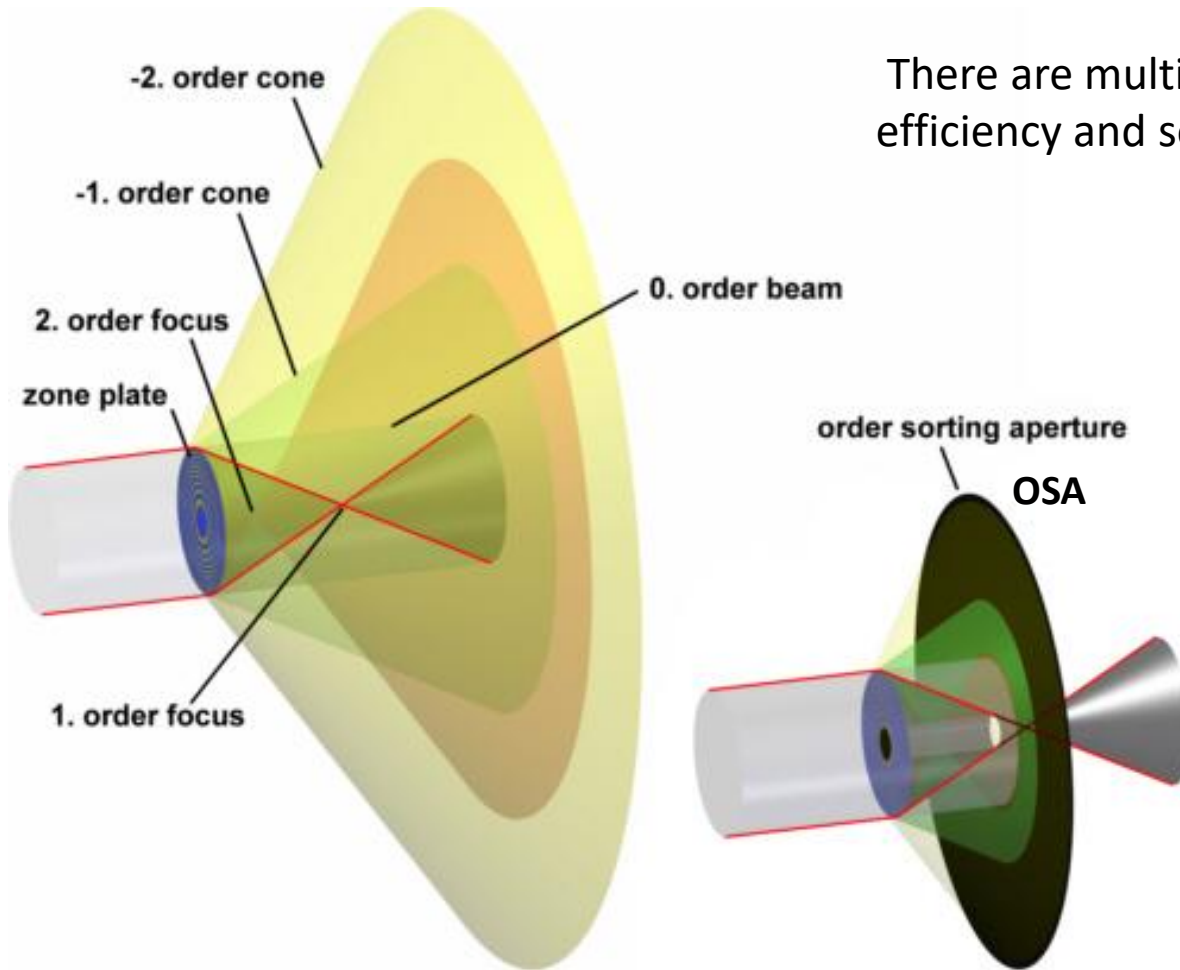
λ , Δr , and N – parameters defining the FZP

N – the number of zones

Focusing and Imaging Zone Plate

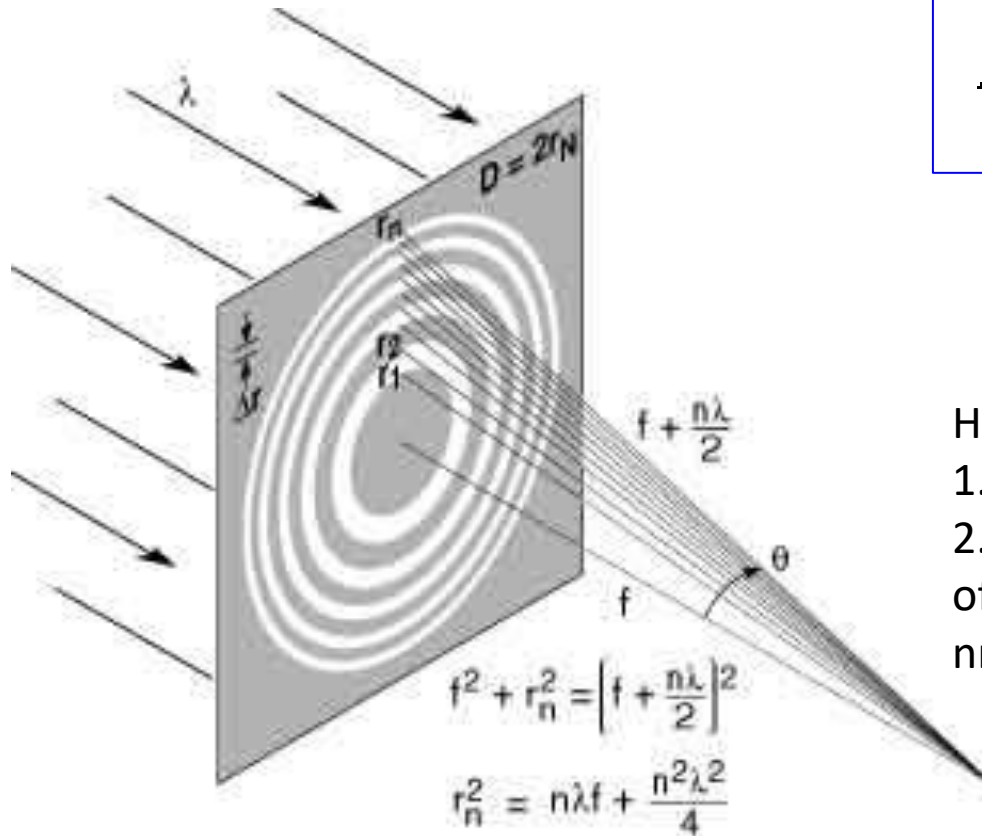
A ZP is a diffractive element which accomplishes in X-ray microscopy the same functions (focusing, imaging) as a glass lens in Visible light Microscopy

The main difference consists in multiple focusing and foci, due to diffraction



There are multiple orders → reduced efficiency and sorting order necessary

Focusing and Imaging Zone Plate



Spatial resolution

$$Res = \frac{0.610\lambda}{NA} = 1.22 \Delta r$$

Numerical Aperture

$$NA = \lambda / 2\Delta r$$

Homework:

1. deduce the NA starting from $NA \sim D/2f$
2. determine the size D and focal length f of a ZP of $N= 1000$ zones, working at $\lambda= 1$ nm with max NA

$$f = 4N(\Delta r)^2 / \lambda$$

$$D = 4N\Delta r$$

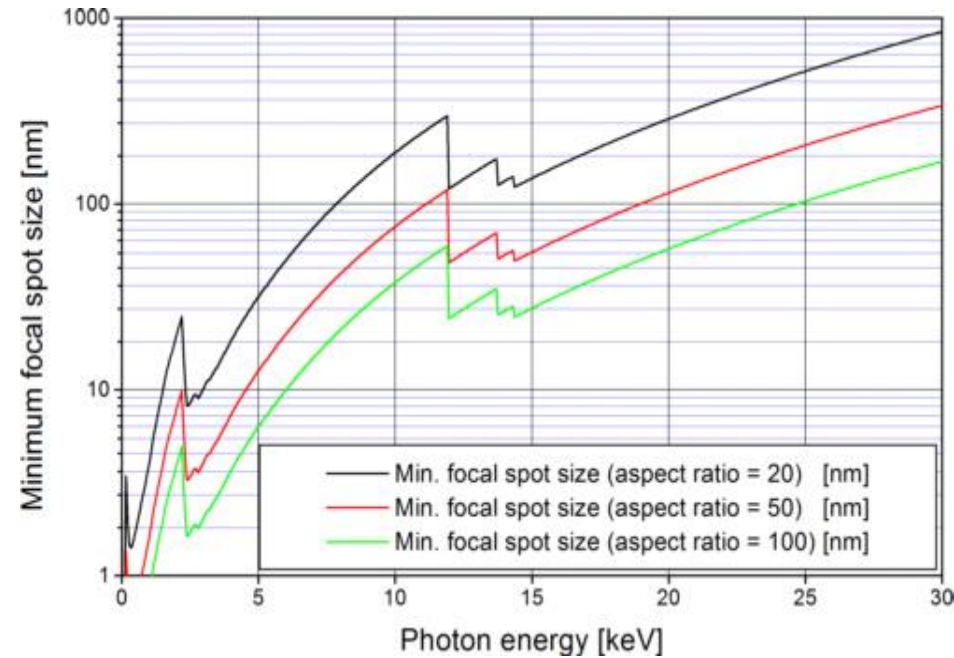
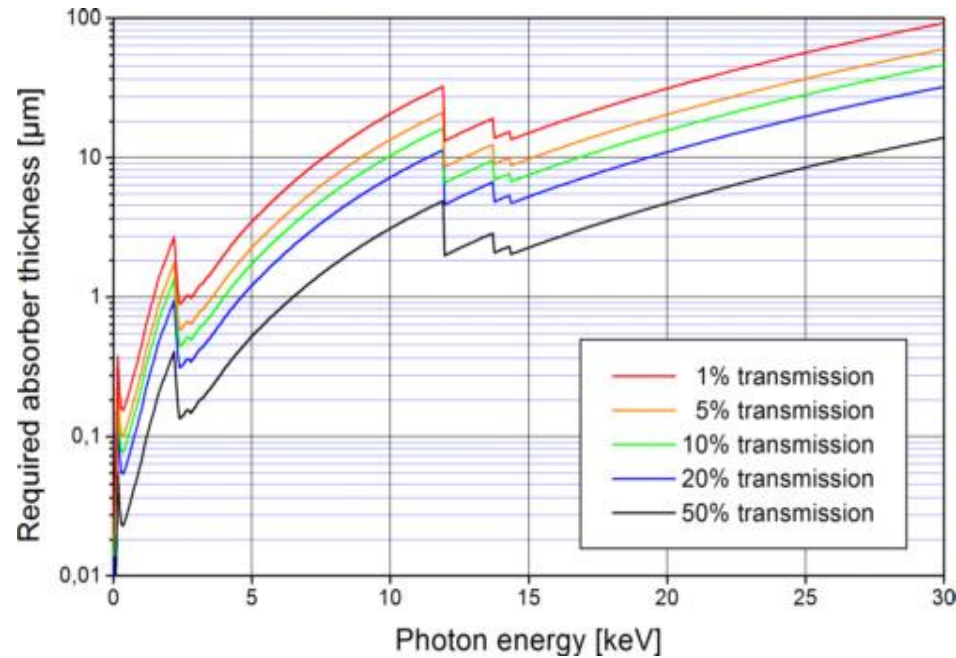
The width of outer zone Δr defines the resolution;
 the width size depends of the fabrication – e-beam 15 nm for X-ray FZP

Some facts about ZP fabrication

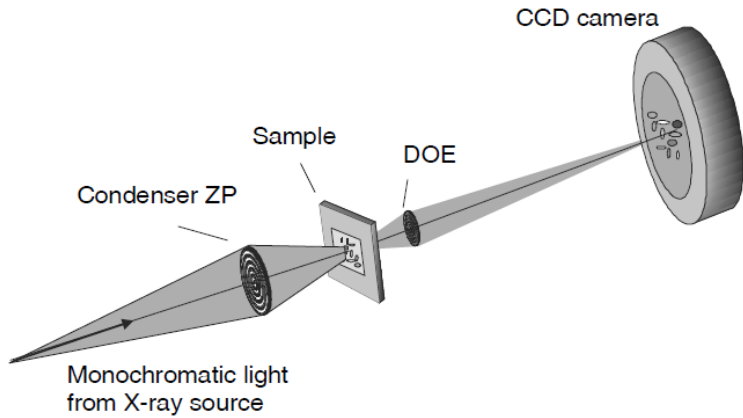
High resolution vs high efficiency \rightarrow high aspect ratio of the zones \rightarrow difficult fabrication (e-beam and deposition)

Gold thickness required to absorb most of the incoming light in the zone plate rings

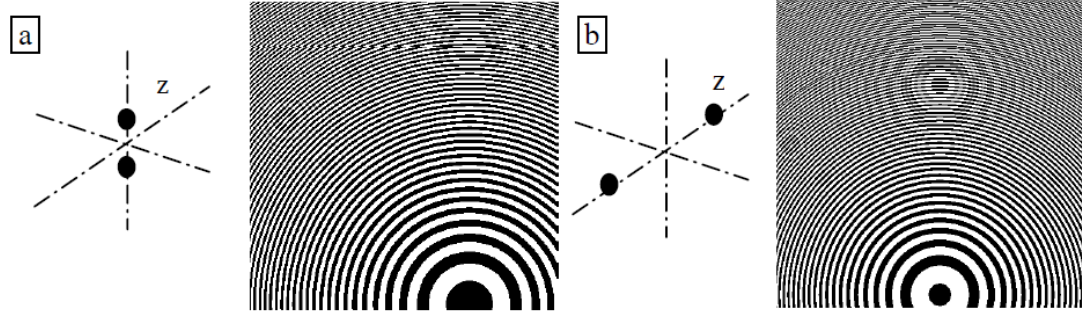
Theoretically minimum achievable spot size when 50% transmission of the gold absorbers is tolerated



X-Ray microscopy Phase contrast with Zone Plates

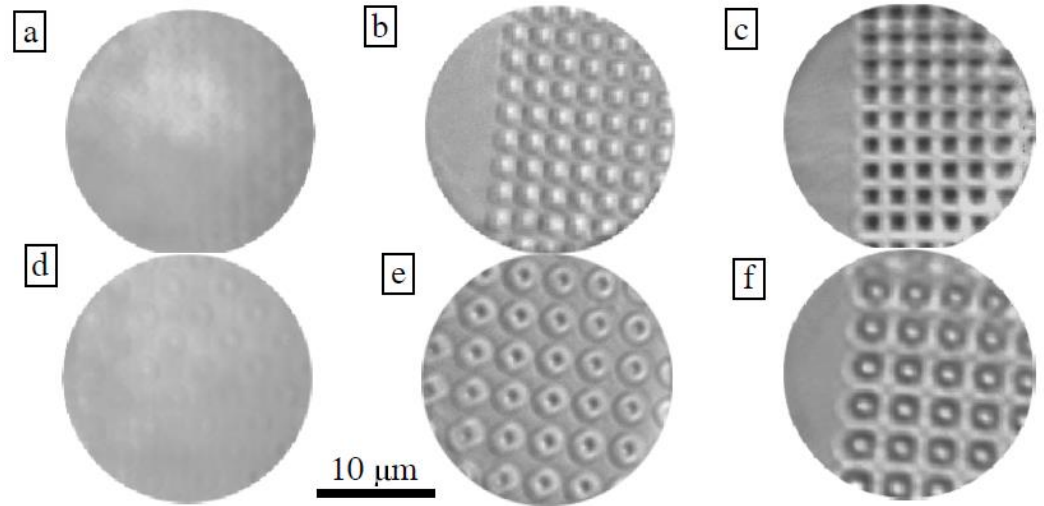
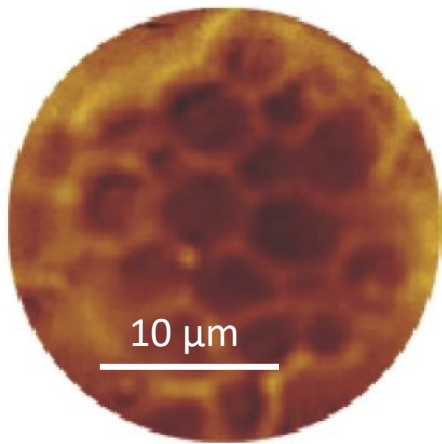


Detail and function of DOE (ZP)



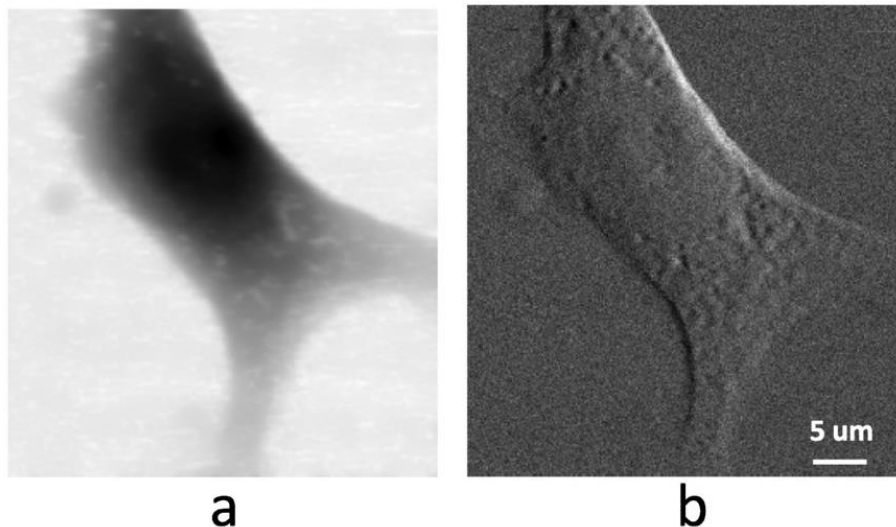
PMMA, 1.5 micron thick sample image
sample transparency > 99 % at 4 keV

Yeast cells image

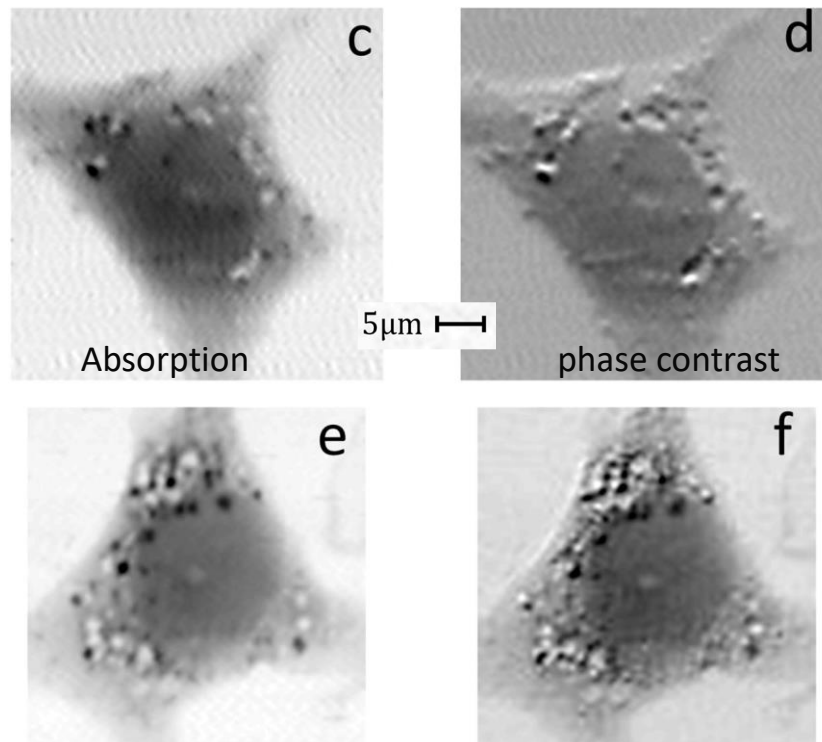


High-resolution scanning transmission soft X-ray microscopy for rapid probing of nanoparticle distribution and sufferance features in exposed cells

Nanotoxicity

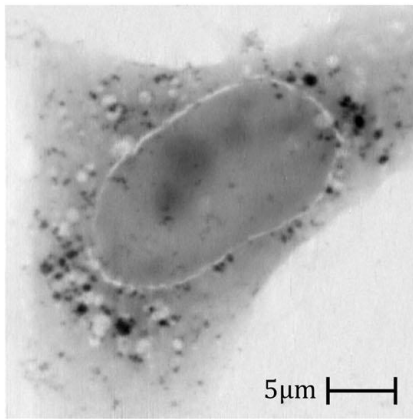


Absorption (a) and phase contrast (b) images of a control fibroblast cell (not exposed to NPs) @900 eV incident photon energy

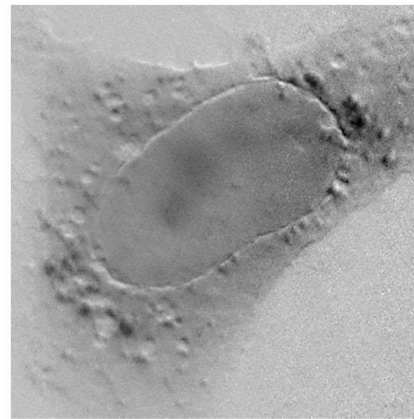


CoFe₂O₄ NPs

Absorption and phase contrast images of fibroblast cells exposed to different CoFe₂O₄ NP concentration: 40 μM (c and d), 250 μM (e and f) 20 ms dwell time / pixel, 900 eV



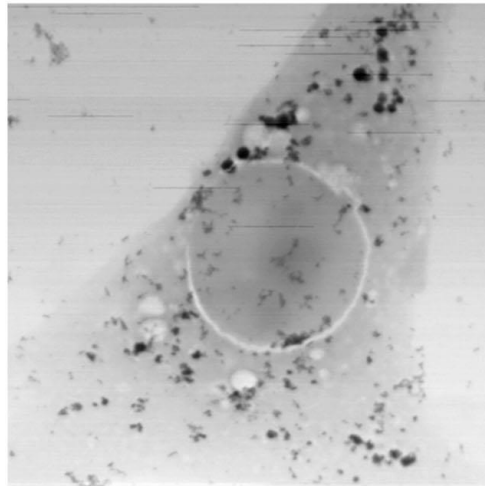
a



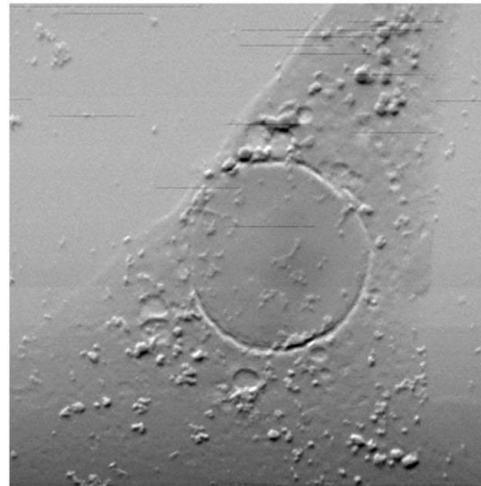
b

Absorption

phase contrast



c



d

Absorption (a, c) and phase contrast (b, d) images of two fibroblast cells to 1000 μM CoFe_2O_4 NP concentration. Imaging parameters: 900 eV (a, b) and 707 eV (corresponding to the L3 Fe edge) (c, d) incident photon energy, 135nm (a, b) and 80 nm (c, d) spot size, 350 ms dwell time/pixel.

$$\lambda \text{ [nm]} = 1.24 / E \text{ [keV]}$$

Radiation Damage

Imaging biological cells with X-rays is challenging due to the composition of the cells themselves, which contain low atomic number constituents such as hydrogen, carbon, oxygen, or nitrogen.

In order to collect sufficient information high flux beams are used. [Flux]=[energy/time/area]

High flux increases the dose to the sample → **radiation damage** :

- Direct radiation damage: the structure of molecules are altered with the possibility of loss of crystallinity to a more amorphous system (e.g., breaking chemical bonds)
- Indirect radiation damage, typically ionization of water produces free radicals that can break chemical bonds or induce oxidation.

Dose – definition for X-rays of energy $h\nu$ and matter with a mass density ρ_m

$$D = \frac{\mu I_0 T h\nu}{\rho_m \sigma}$$

the dose D in units of Gray ($\text{Gy} = \text{Jkg}^{-1} = \text{m}^2 \text{s}^{-2}$);

I_0 - the primary beam intensity in photons/s,

T - the exposure time in seconds,

σ - the exposed area per scan point or exposure in m^2

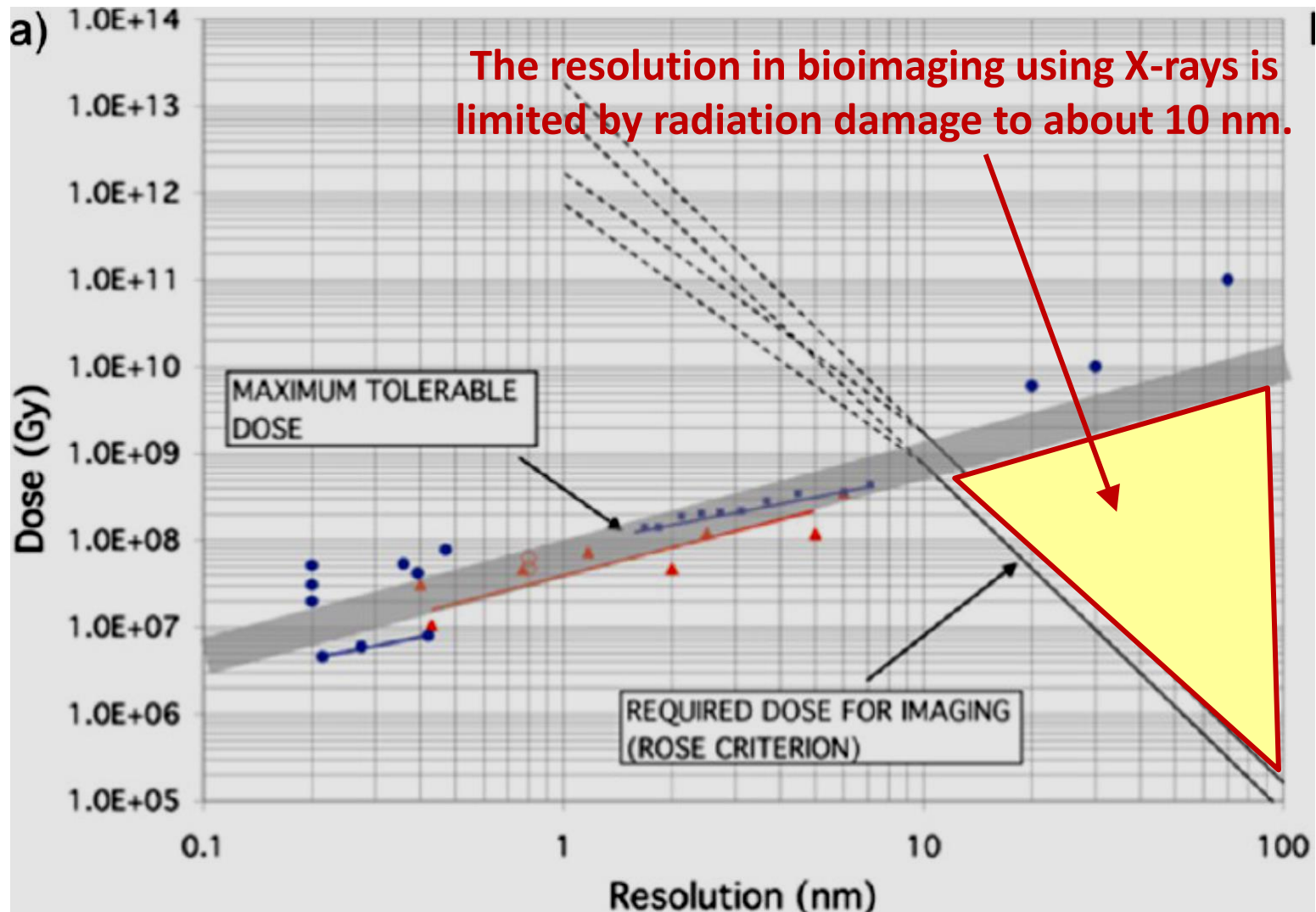
Rule of thumb:

The maximum tolerable dose (in Gy) to achieve a resolution between 0.1 and 10 nm is

$$D_{\text{tot}} = 108 \text{ Gy nm}^{-1} \times \text{resolution (in nm)}$$

Routine radiation doses to patients, medical staff, and industrial radiation workers are below 100 mGy !

Dose dependence of the resolution for X-ray imaging

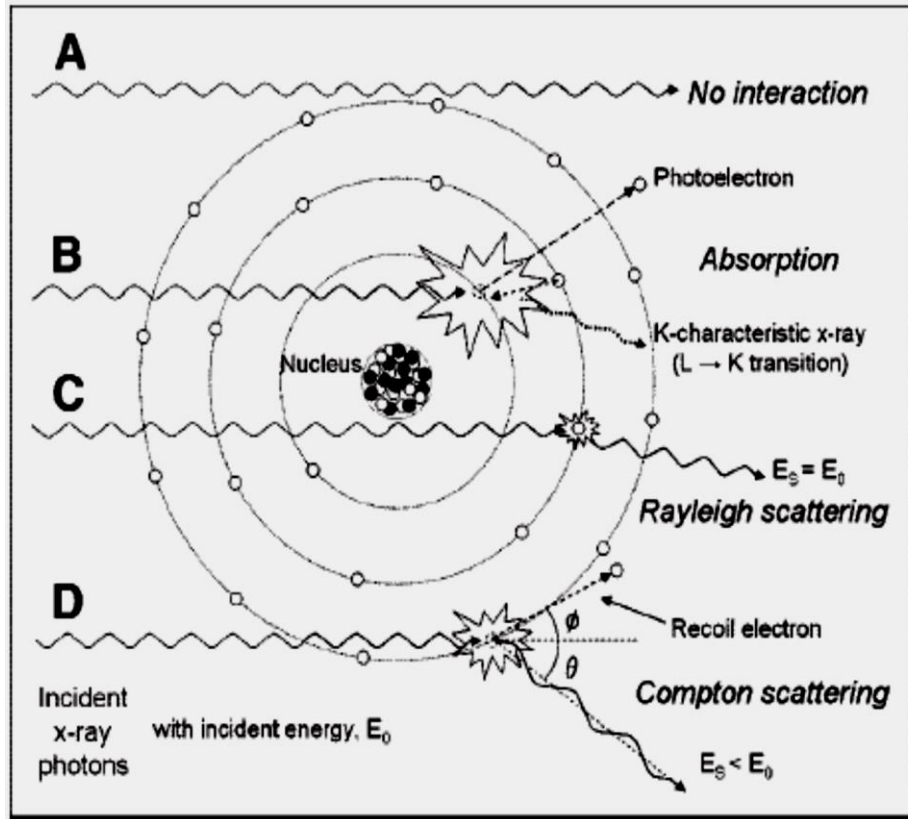


DOI: 10.1021/acsnano.7b03447, ACS Nano 2017, 11, 8542–8559 Review

Howells, M. R et al An Assessment of the Resolution Limitation Due to Radiation-Damage in X-Ray Diffraction Microscopy. J. Electron Spectrosc. Relat. Phenom. 2009, 170, 4–12

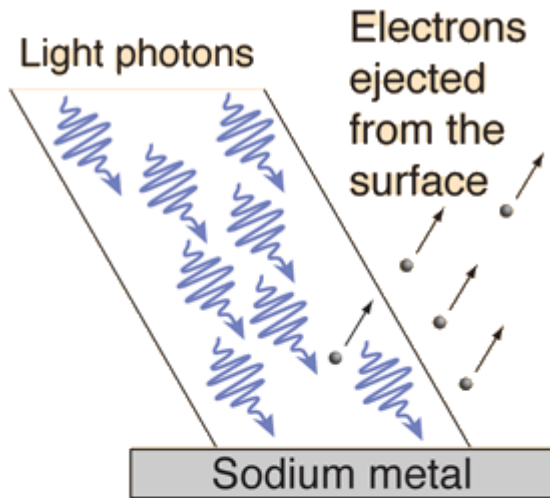
X-ray – sample interactions

possible contrast mechanisms



(A) Primary, unattenuated beam does not interact with material.

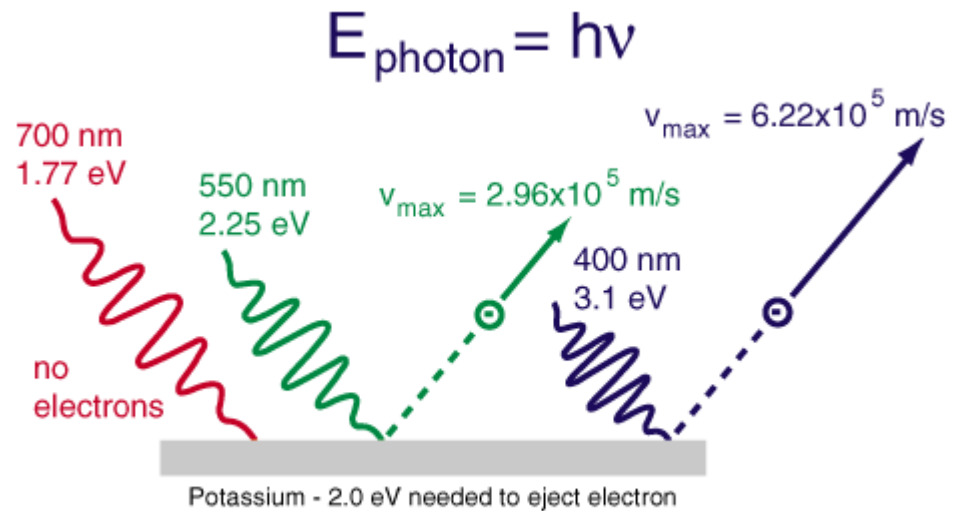
(B) Photoelectric absorption involves the interaction of an incident x-ray photon with an inner shell electron in the absorbing atom that has a binding energy similar to but less than the energy of the incident photon. The incident x-ray photon transfers its energy to the electron and results in the ejection of the electron from its shell (usually the K shell) with a kinetic energy equal to the difference of the incident photon energy, E_0 , and the electron shell binding energy, E_{BE} . The vacated electron shell is subsequently filled by an electron from an outer shell with less binding energy (e.g., from the L or M shell), producing a characteristic x-ray equal in energy to the difference in electron binding energies of the source electron shell and the final electron shell. If the x-ray energy is equal to the electronic binding energy ($E_0 = E_{BE}$), the photoelectric effect becomes energetically feasible and a large increase in attenuation occurs.



Photon energy

$$E = h\nu$$

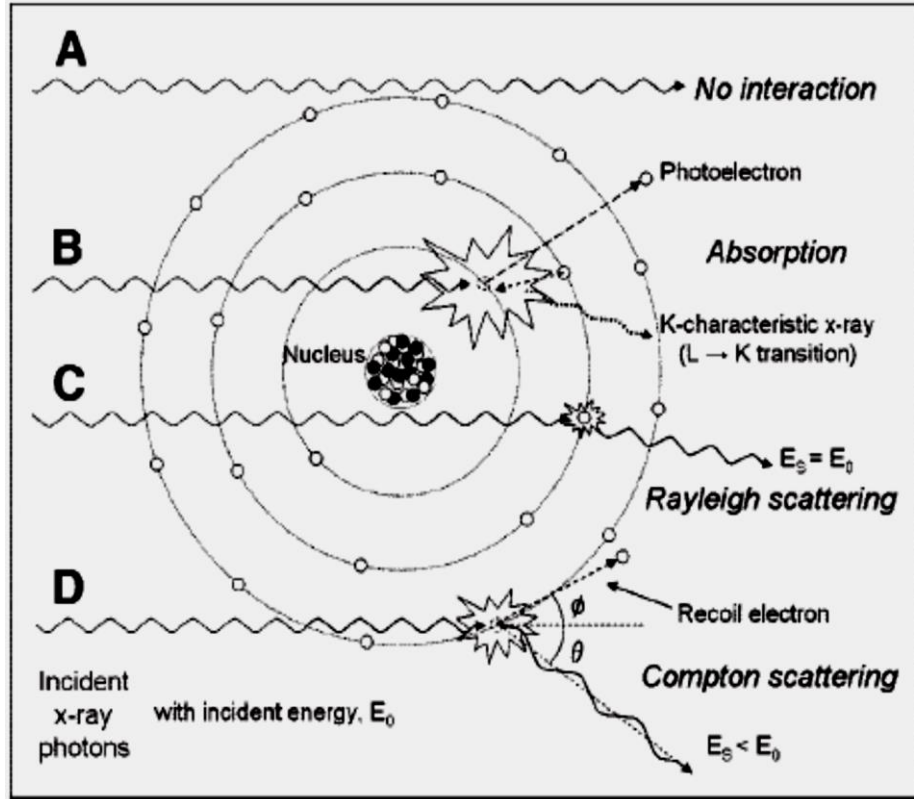
explains the experiment and shows that light behaves like particles.



Photoelectric effect

X-ray – sample interactions

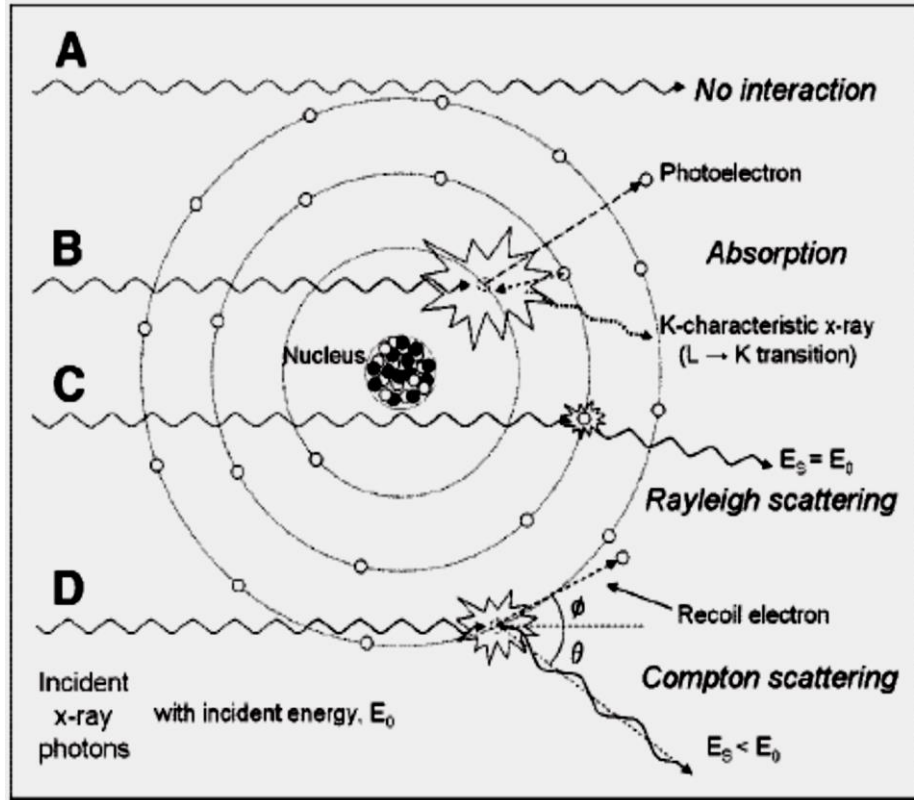
possible contrast mechanisms



(C) An incident x-ray photon can interact with an electron and be deflected (scattered) with no loss in energy. This process is also known as coherent or elastic scattering, and it occurs by temporarily raising the energy of the electron without removing it from the atom. The electron returns to its previous energy level by emitting an x-ray photon of equal energy but with a slightly different direction. There is no absorption of energy, and the majority of the x-ray photons are scattered with a small angle. In soft tissue, Rayleigh scattering probability is low, on the order of 5% of all scattering events, because of the low effective atomic number of soft tissues ($Z \sim 7.5$). The possibility of Rayleigh scattering increases with increasing Z of the absorbed atom and decreasing x-ray energy.

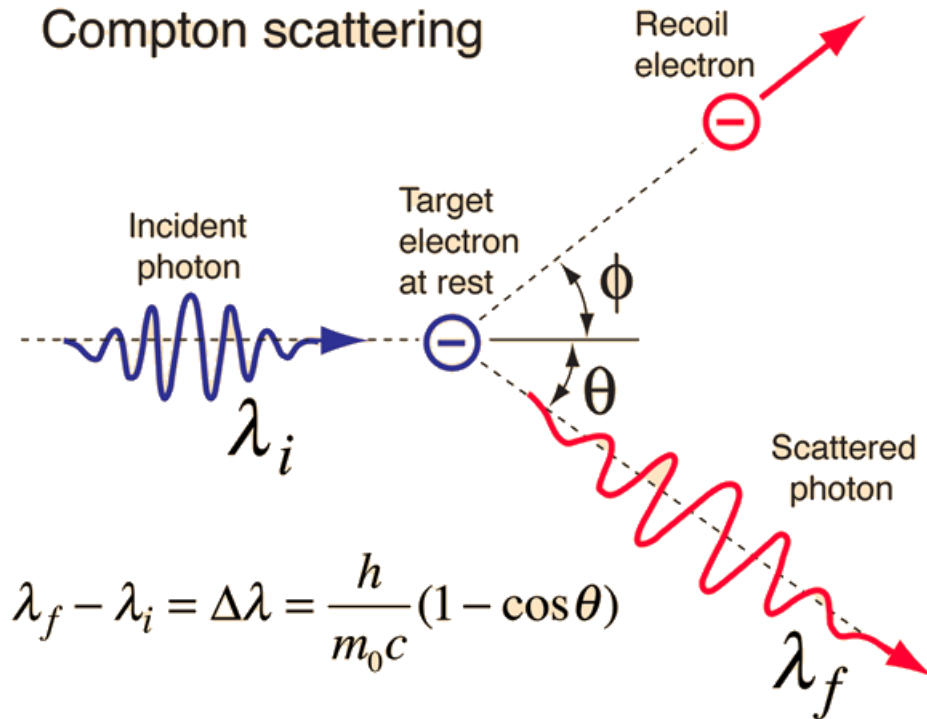
X-ray – sample interactions

possible contrast mechanisms



(D) Compton scattering is an inelastic interaction between an x-ray photon of energy E_0 that is much greater than the binding energy of an atomic electron (in this situation, the electron is essentially regarded as “free” and unbound). Partial energy transfer to the electron causes a recoil and removal from the atom at an angle, ϕ . The remainder of the energy, E_s , is transferred to a scattered x-ray photon with a trajectory of angle θ relative to the trajectory of the incident photon. While the scattered photon may travel in any direction (i.e., scattering through any angle θ from 0° to 180°), the recoil electron may only be directed forward relative to the angle of the incident photon (0° to 90°).

Compton scattering



Compton scattering interaction occurs with essentially unbound electrons, with transfer of energy shared between recoil electron and scattered photon, with energy exchange.

The scattering of photons from charged particles

Absorption of an x-ray photon with sufficient energy ejects an electron, producing a short-lived core hole. In addition to the direct measurement of absorption amplitudes, x-ray emission spectroscopy relies on the physical phenomena that accompany **absorption events**.

X-ray photoelectron spectroscopy (XPS) captures the primary ejected electrons and secondary electrons resulting from the de-excitation process. The first step of the de-excitation process is transition of an electron from a higher shell into the electron hole vacancy. The second step is a release of the energy difference, E , via one of two processes:

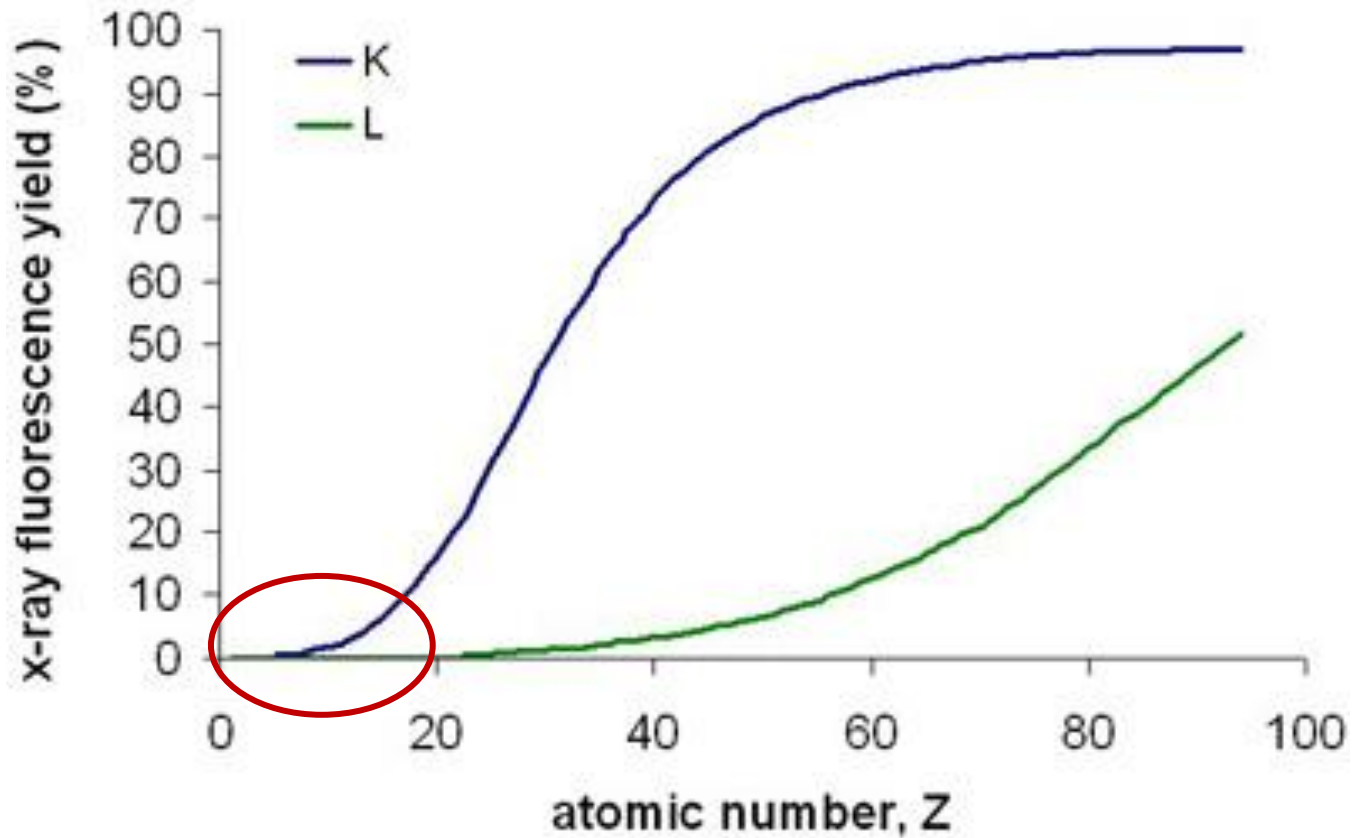
- (i) emission of so-called **Auger electrons** with energy equal to or lower than E and
- (ii) emission of **photons** with energy equal to E , called fluorescence

Auger emission dominates for photon energies below 1 keV, whereas the fluorescence photon emission dominates for higher photon energies and the ratio of fluorescence to Auger events is described by the **fluorescence yield**.

The fluorescent spectra of a given element are well defined by the energy states of the atom and the selection rules for allowed transitions, so the elemental content of a specimen can be determined by x-ray fluorescence microscopy.

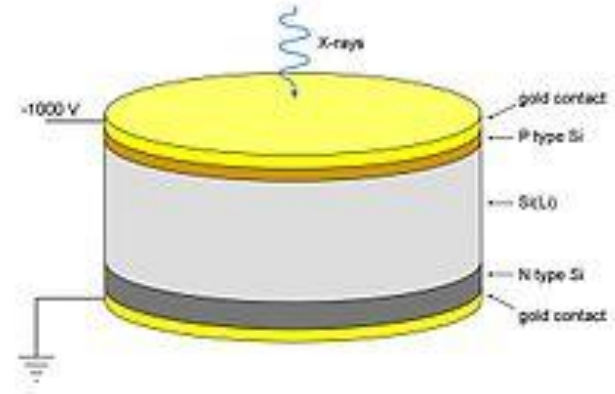
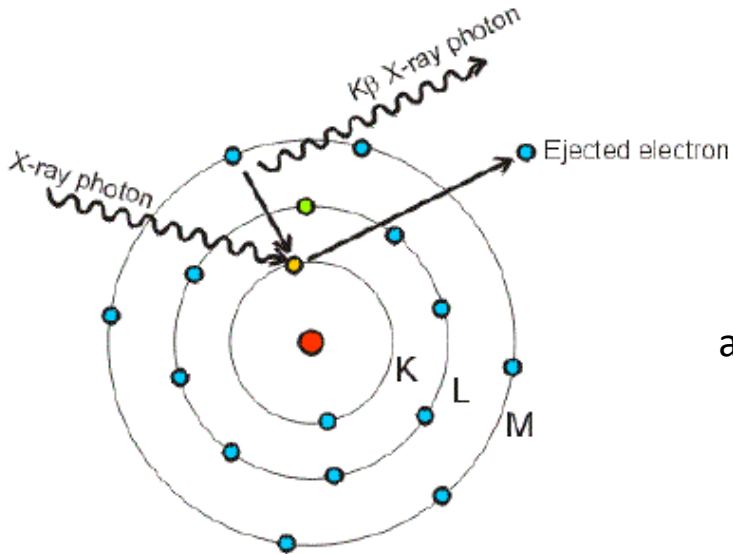
The K and L **fluorescence yield** as a function of atomic number, Z .

the yield for the light elements is very low \rightarrow low sensitivity for these elements.



X-ray fluorescence

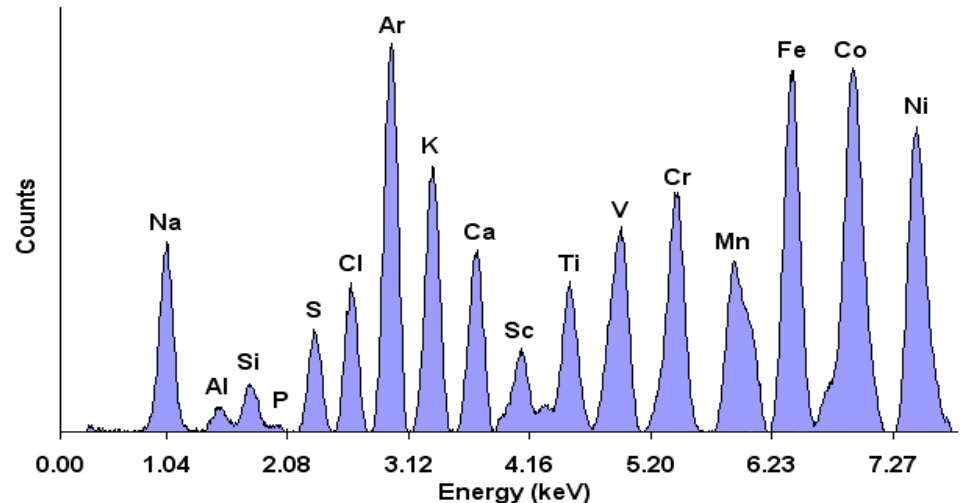
Energy dispersive X-ray fluorescence detector



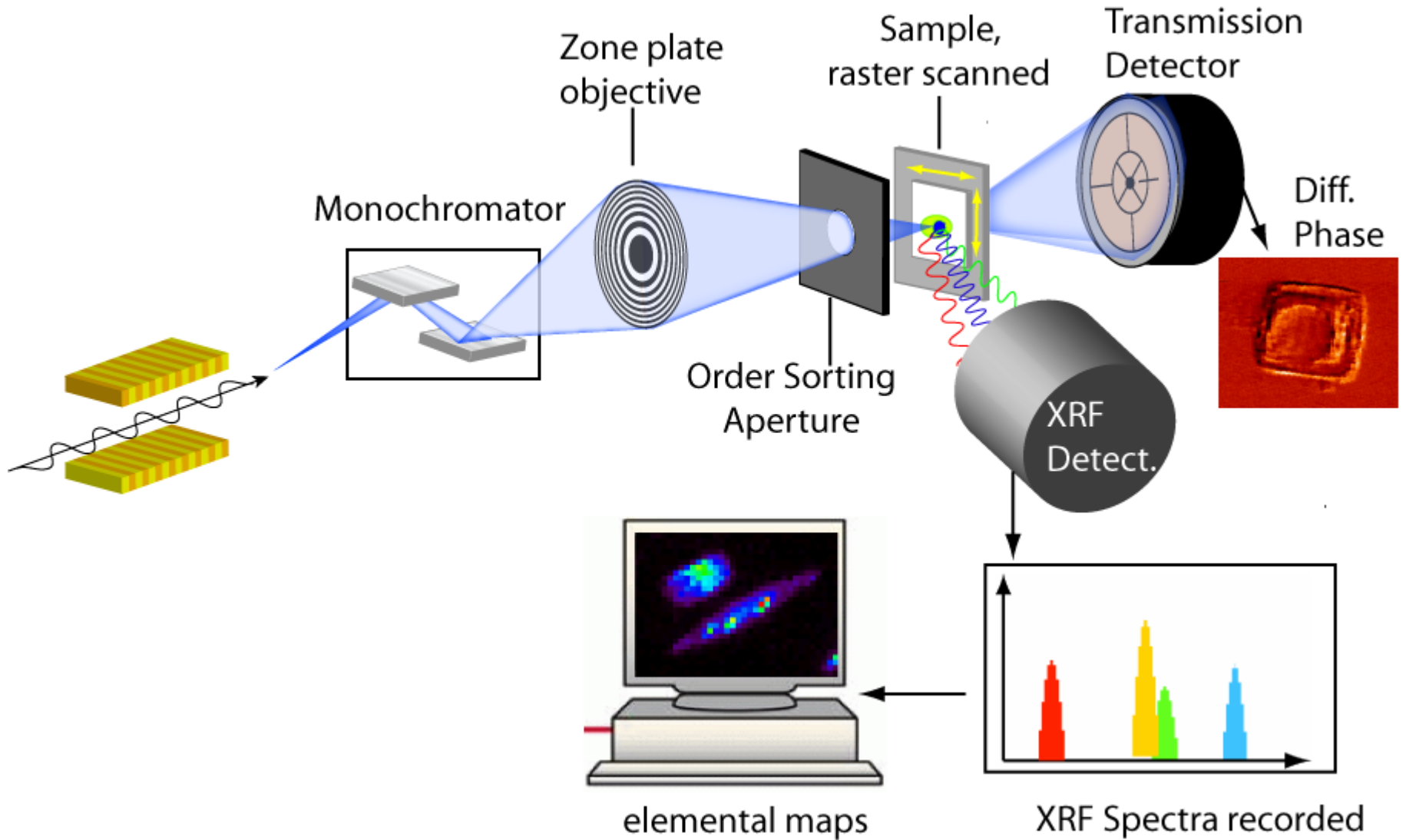
an X-ray photon incident upon the Si(Li) diode will give up its energy to form electron-hole pairs, the number of which is proportional to the energy of the photon

As in the case of e^- in x-ray sources X-rays may kick off one electron from a deep level and originate x-ray emission

Low Energy Fluorescence with the XR100CR



X-ray fluorescence



A fluorescence detector can detect (for instance) instance traces of metal in biological systems

X-Ray microspectroscopy

Additional chemical information can be obtained by a careful measurement of detailed absorption fluctuations surrounding the selected atomic edge.

X-ray absorption spectroscopy typically covers the immediate absorption edge region of a few 10 eV and can extend to energies hundreds of eV above the edge.

Depending on the energy range the absorption spectroscopy is divided into two regimes:

- x-ray absorption near-edge spectroscopy (XANES) or near edge x-ray absorption fine structure (NEXAFS), which provides information about the chemical state and bonding configuration of the absorbing atom
- extended x-ray absorption fine-structure spectroscopy (EXAFS), which is used to determine the coordination and bond distances to the neighboring atoms

Kaulich et al J. Phys.: Condens. Matter 2010

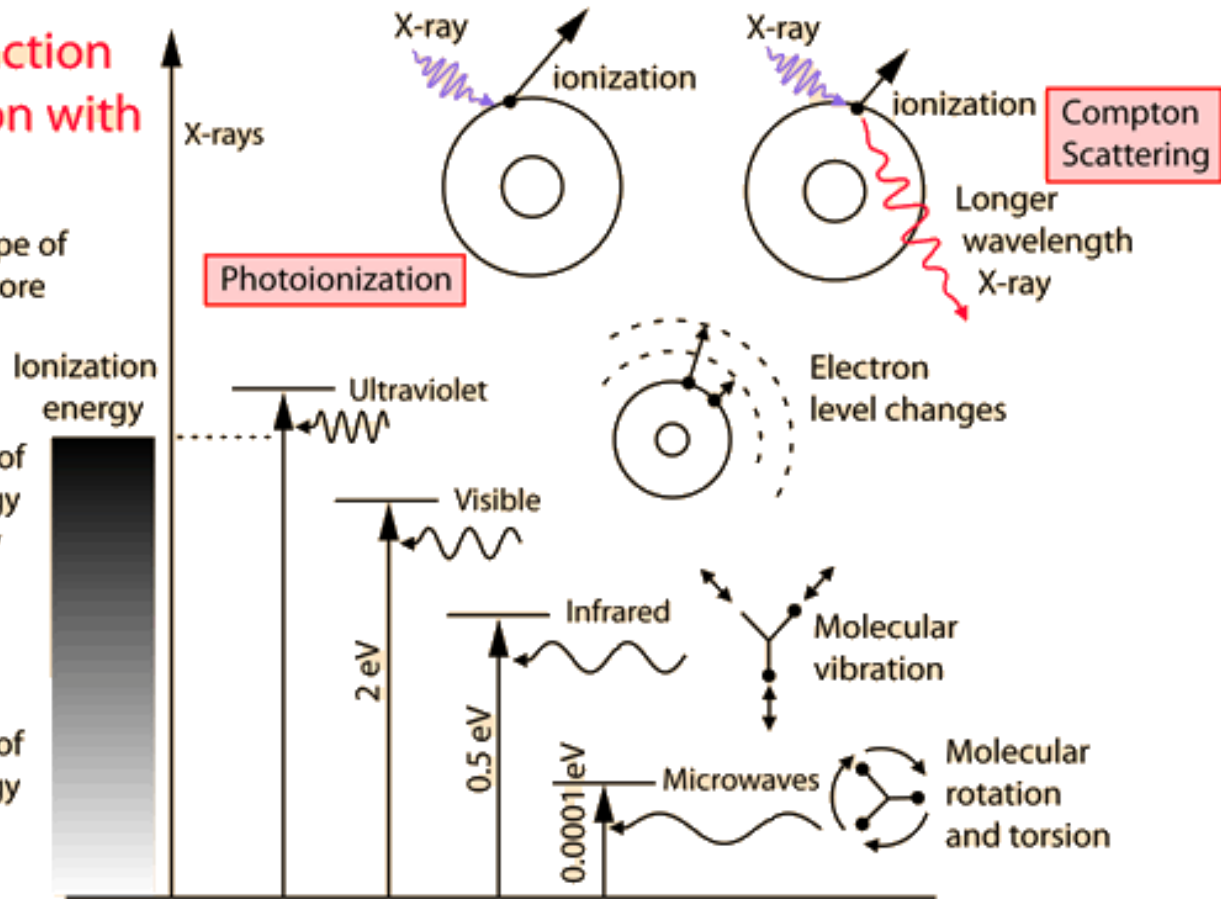
<https://indico.ictp.it/event/a11156/session/49/contribution/30/material/1/2.pdf>

The interaction of radiation with matter.

Click on any type of radiation for more information.

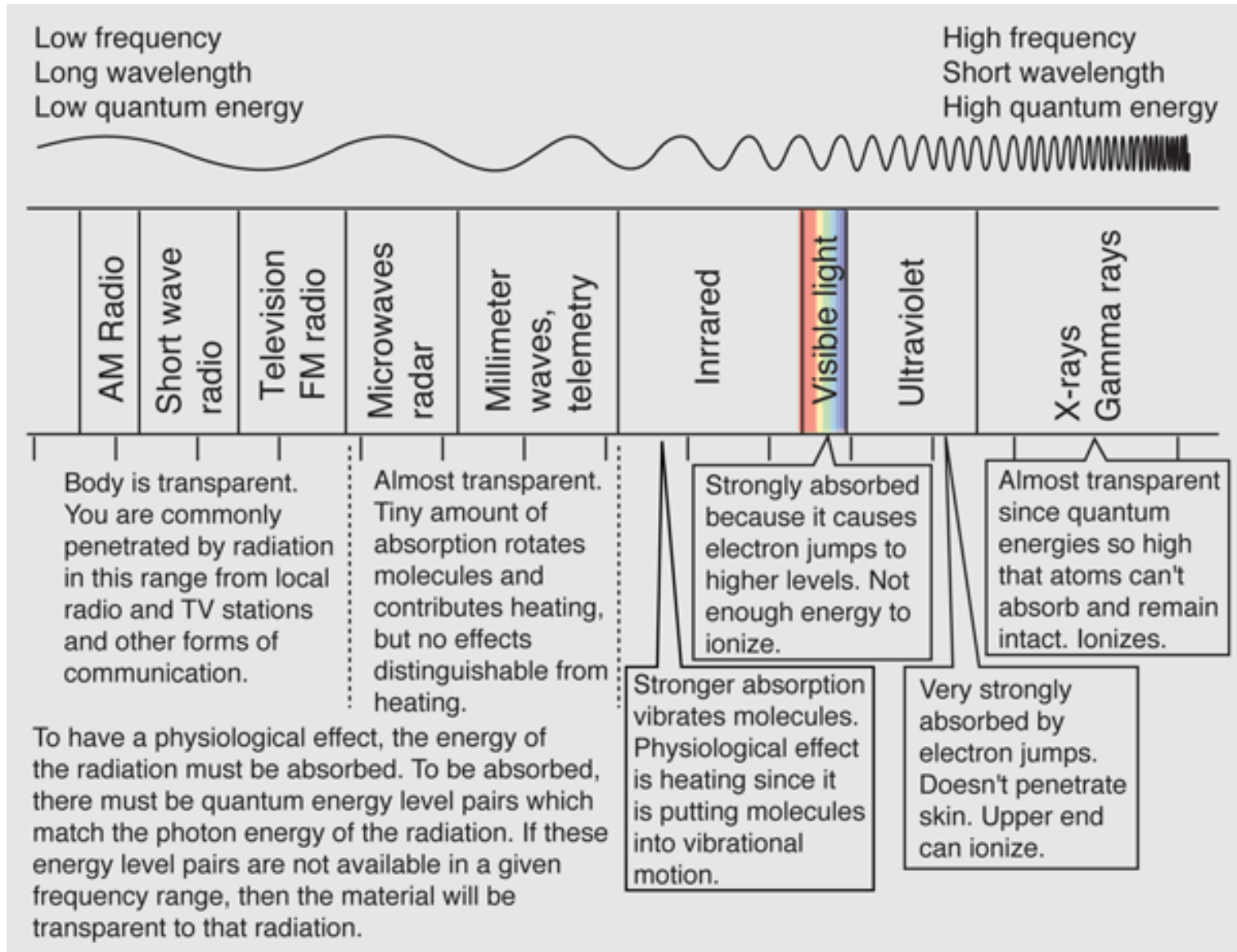
Large number of available energy states, strongly absorbed.

Small number of available energy states, almost transparent.



<http://hyperphysics.phy-astr.gsu.edu/hbase/mod3.html#c1>

Electromagnetic spectrum annotated with physiological effects



X-Ray microscopy (and micro-spectroscopy) with Synchrotron light

Synchrotron radiation – radiation emitted from charged particles traveling at relativistic speeds

How is synchrotron light created? Acceleration of a charged particle causes it to give off energy as photons.

Electrons are generated by the electron gun (1) in the centre of the synchrotron and accelerated to 99.9997% of the speed of light by the linear accelerator, or linac (2).

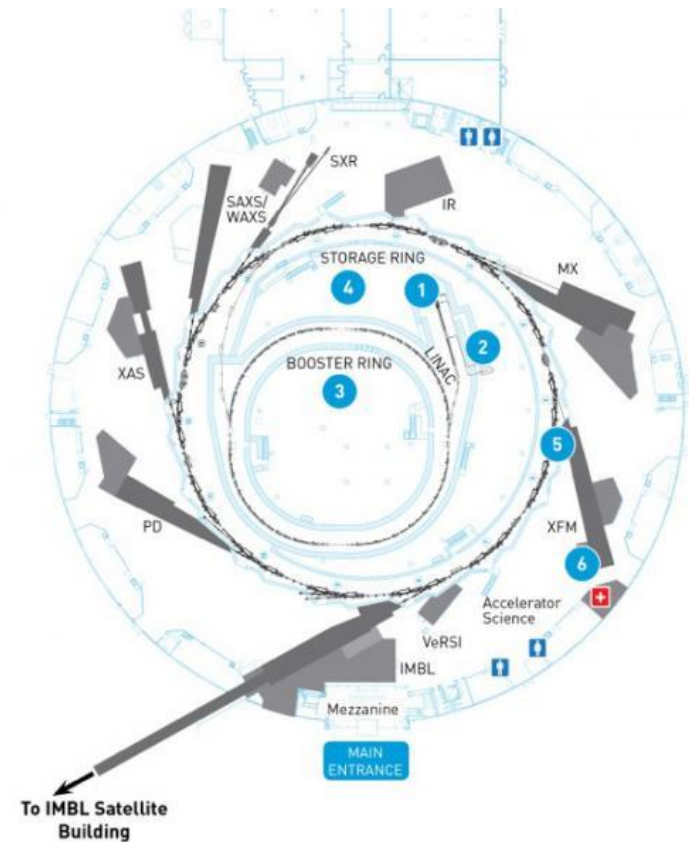
The electrons are then transferred to the booster ring (3), where they are increased in energy from 100 MeV to 3,000 MeV (or 3 GeV) in about half a second.

They are then transferred to the outer storage ring (4).

The electrons are circulated around the storage ring by a series of magnets separated by straight sections.

As the electrons are deflected through the magnetic field created by the magnets, they give off electromagnetic radiation, so that at each bending magnet a beam of synchrotron light is produced.

This electromagnetic radiation produced by the synchrotron is emitted in a narrow cone in the forward direction, at a tangent to the electron's orbit.



Synchrotron radiation covers the entire EM spectrum, X-ray is of the most interest.

What makes synchrotron light unique?

Synchrotron light is unique in its intensity and brilliance.

The **synchrotron light is as bright as 1 million Suns !!!** What is **brilliance** ? 

Properties of synchrotron light:

- **High brightness:** synchrotron light is extremely intense (hundreds of thousands of times more intense than that from conventional x-ray tubes) and highly collimated.
- **Wide energy spectrum:** synchrotron light is emitted with energies ranging from infrared light to hard x-rays.
- **Tunable:** it is possible to obtain an intense beam of any selected wavelength.
- **Highly polarised:** the synchrotron emits highly polarised radiation, which can be linear, circular or elliptical.
- **Emitted in very short pulses:** pulses emitted are typically less than a nano-second (a billionth of a second), enabling time-resolved studies.

<https://www.ansto.gov.au/education/nuclear-facts/what-is-synchrotron-light>

<https://www.elettra.trieste.it/lightsources/elettra/machine.html>

<https://indico.ictp.it/event/a11156/session/49/contribution/30/material/0/0.pdf>

What is brightness ?

Definition of the spectral flux and the brightness :

$$\mathcal{F} = \frac{\text{Number of photons}}{(\text{sec}) (0.1\% \text{ bandwidth})}$$

Beam collimation

Size of beam source

$$\mathcal{B} = \frac{\text{Number of photons}}{(\text{sec}) (\text{mm}^2) (\text{mrad}^2) (0.1\% \text{ bandwidth})}$$

monochromaticity

SUN Luminosity and Brightness

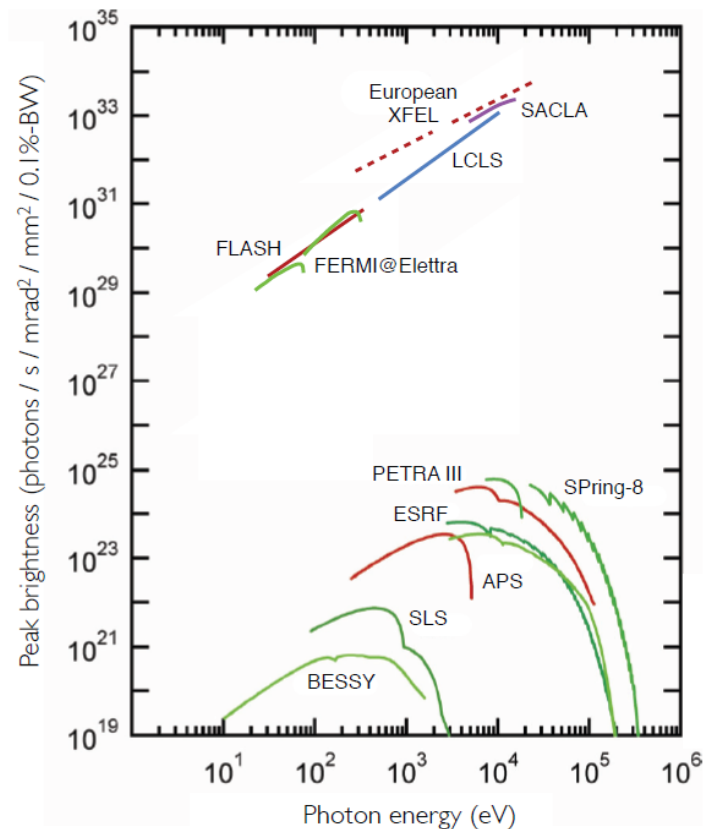
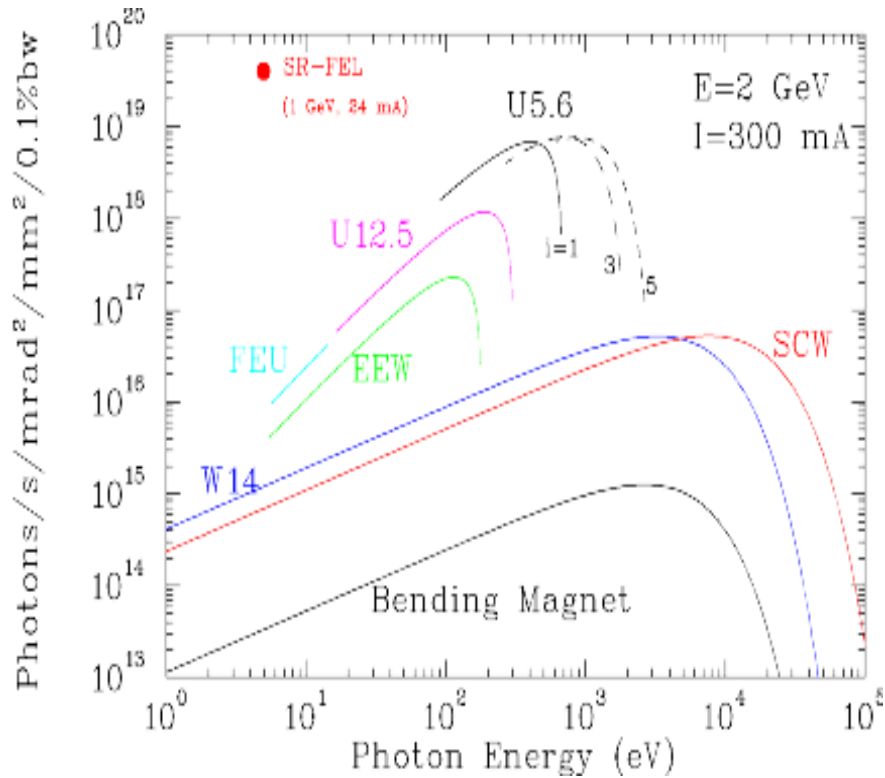
Luminosity = the amount of energy emitted by an object in a unit of time

Absolute measure of radiant power, i.e. it does not depend of observer's distance from object

Luminosity of Sun $L = 3.846 \times 10^{26}$ Watts; apparent Brightness $L = B 4\pi d^2$; d-distance to Sun

Diameter $D = 1.4 \times 10^6$ km , $1 \text{ J} = 2.5 \times 10^{19}$ ph at 500 nm, $d = 150 \times 10^6$ km

Elettra is the third generation storage ring (2 and 2.4 GeV) that has been in operation since October 1993. It has been optimised to provide the scientific community with photons in the energy range from several tens of KeV with spectral brightness of up to 10^{19} photons/s/mm²/mrad²/0.1%bw

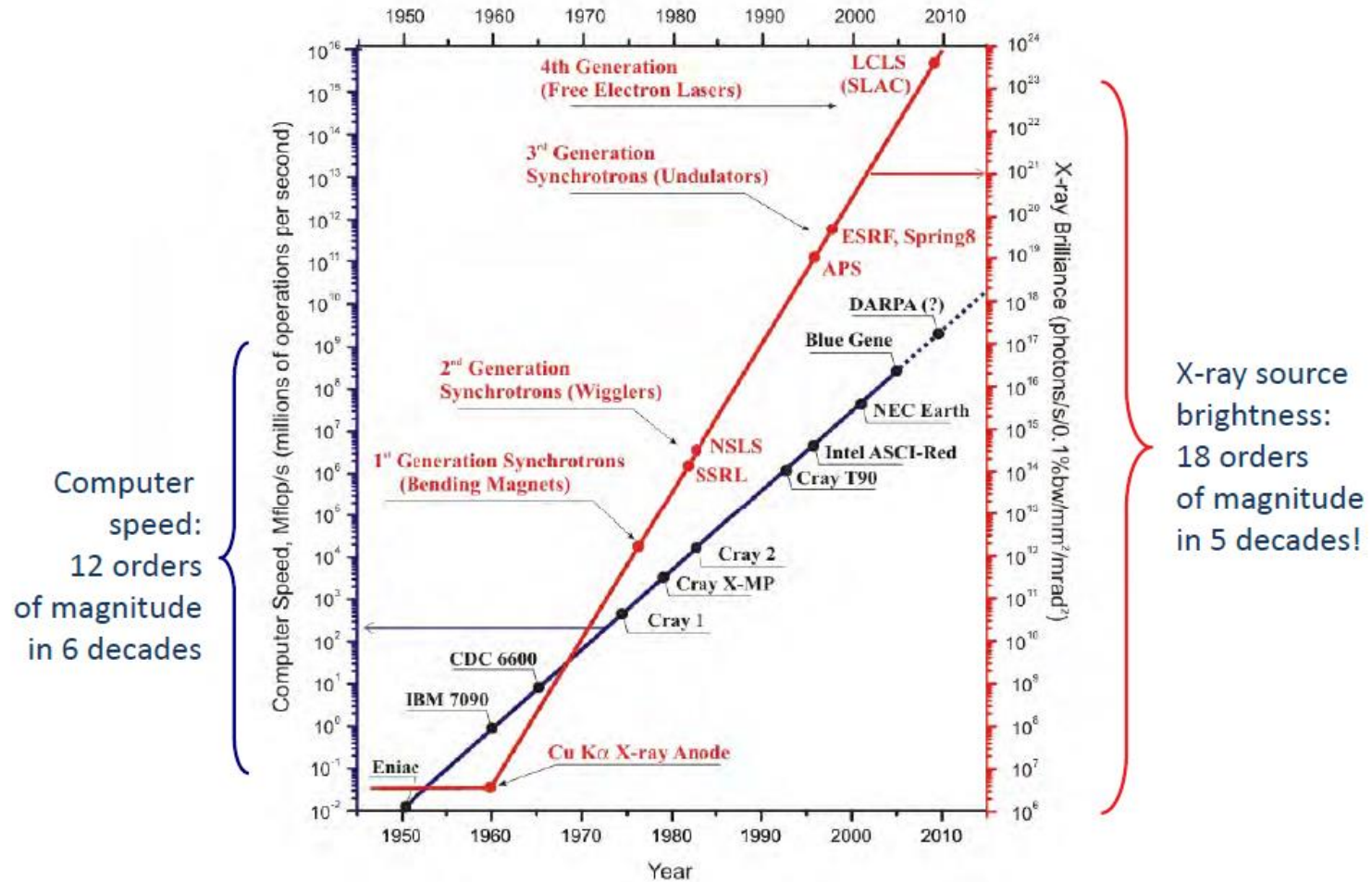


www.elettra.trieste.it/lightsources/elettra/machine.html

Peak spectral brightness (brilliance) of third and fourth generation accelerator-based light sources

How fast Synchrotron technology evolves vs computer technology

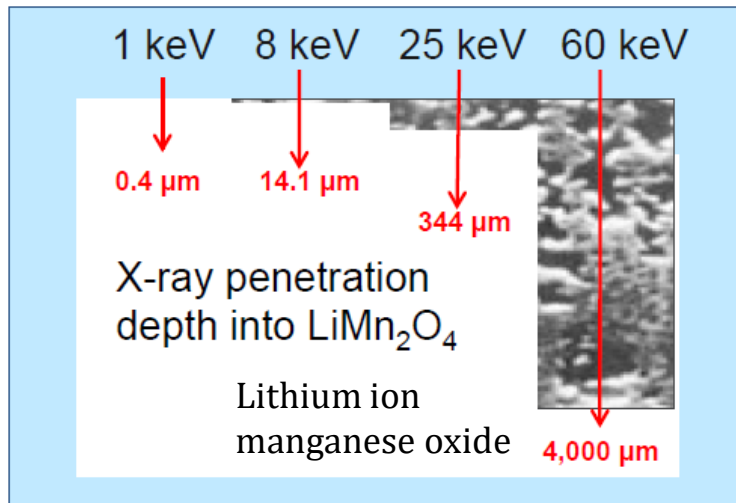
Moore's Law for X-ray Source Brightness



High energy: Necessary to probe deeply into real materials in realistic environments

High-energy x-rays enable deep penetration, making it possible to probe:

- Samples behind thick-walled chambers of reaction vessels
- Buried structures in real materials
 - Turbine blades, commercial batteries
- Materials in extreme conditions, including high pressure, high temperatures

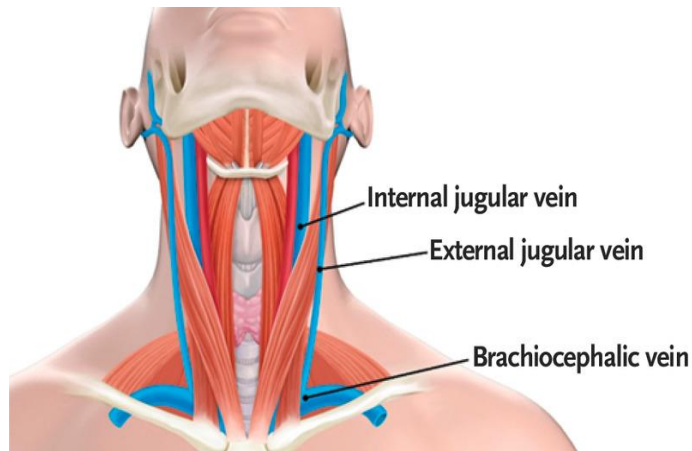


TYPES OF SYNCHROTRON X-RAY METHODS

- Scattering and Diffraction
 - Very high resolution
 - Penetration into sample can be tuned by the incidence angle
 - Tunable wavelength: anomalous scattering - element specific
 - High energy - penetrating
 - Dynamical scattering
 - Small-angle scattering
 - Magnetic scattering
- Spectroscopy
 - Penetration into sample can be tuned by the incidence angle
 - Fluorescence
 - X-ray absorption fine structure
 - Inelastic scattering
- Microscopy and Imaging
- Time-Resolved Measurements

Examples of Xray microscopy applications to cell and tissue imaging

Calcium micro-depositions in jugular truncular venous malformations revealed by Synchrotron-based XRF imaging

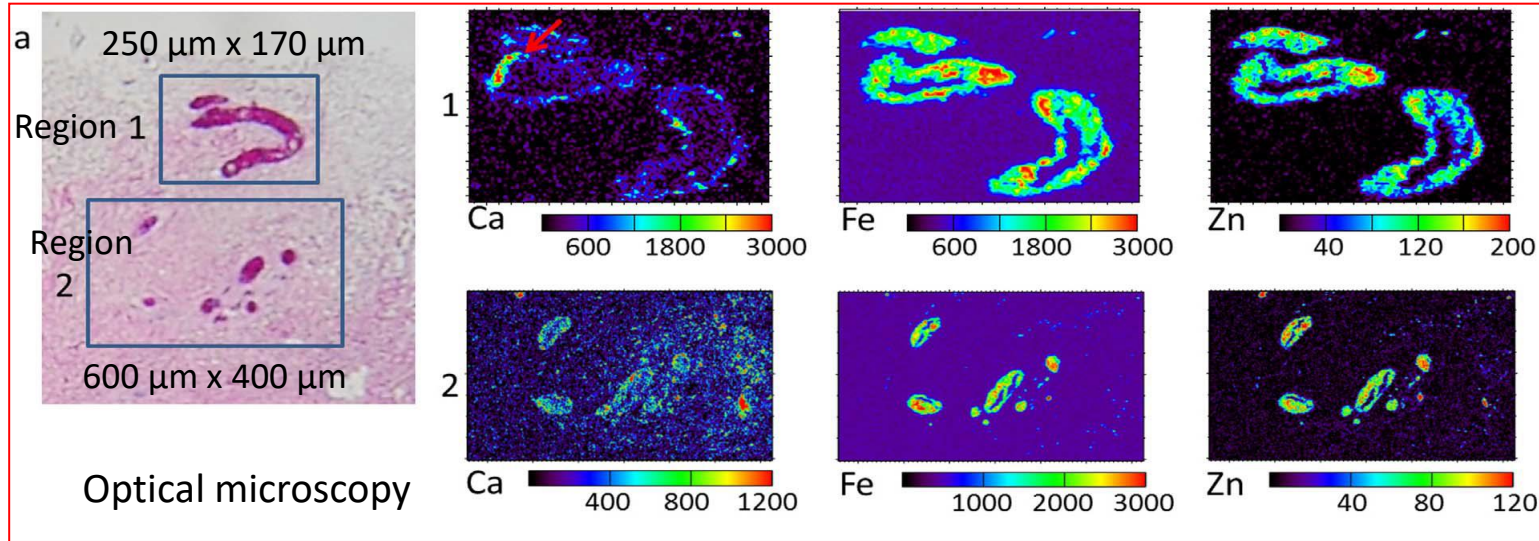


The internal jugular vein may exhibit abnormalities classified as truncular venous malformations (TVMs). Investigating possible morphological and biochemical anomalies at jugular tissue level could help to better understand the link between brain venous drainage and neurodegenerative disorders, recently found associated with jugular TVMs.

Authors performed sequential X-ray Fluorescence (XRF) analyses on jugular tissue samples from TVM patients, using complementary energies at three different synchrotrons. This investigation, coupled with conventional histological analyses, revealed anomalous micro-formations in the pathological tissues and allowed the determination of their elemental composition. Rapid XRF analyses on large tissue areas at 12.74 keV showed an increased Ca presence in the pathological samples, mainly localized in tunica adventitia microvessels. Investigations at lower energy demonstrated that the high Ca level corresponded to micro-calcifications, also containing P and Mg.

Advanced synchrotron XRF micro-spectroscopy is an important analytical tool in revealing biochemical changes, which cannot be accessed by conventional investigations

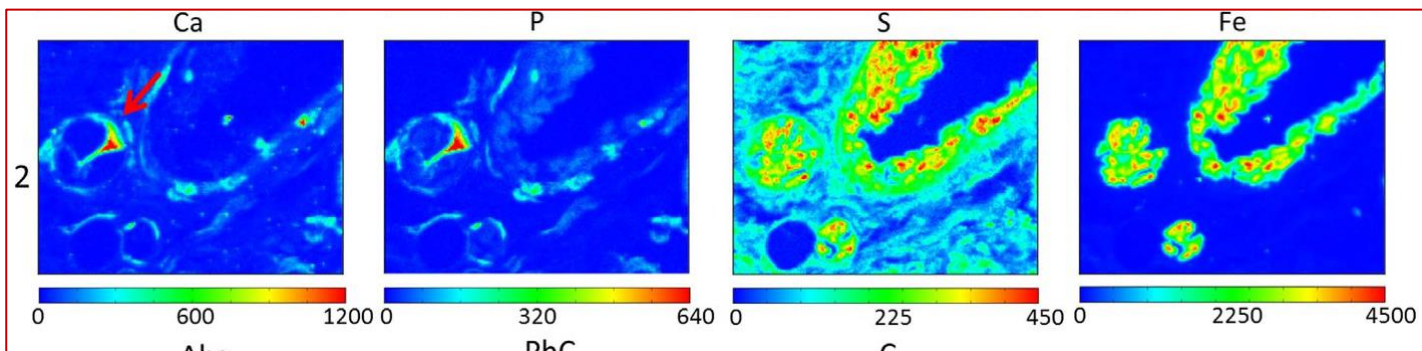
Calcium micro-depositions in jugular truncular venous malformations revealed by Synchrotron-based XRF imaging



X-ray Fluorescence Microscopy (XFM) in multiple sclerosis tissue jugular sections

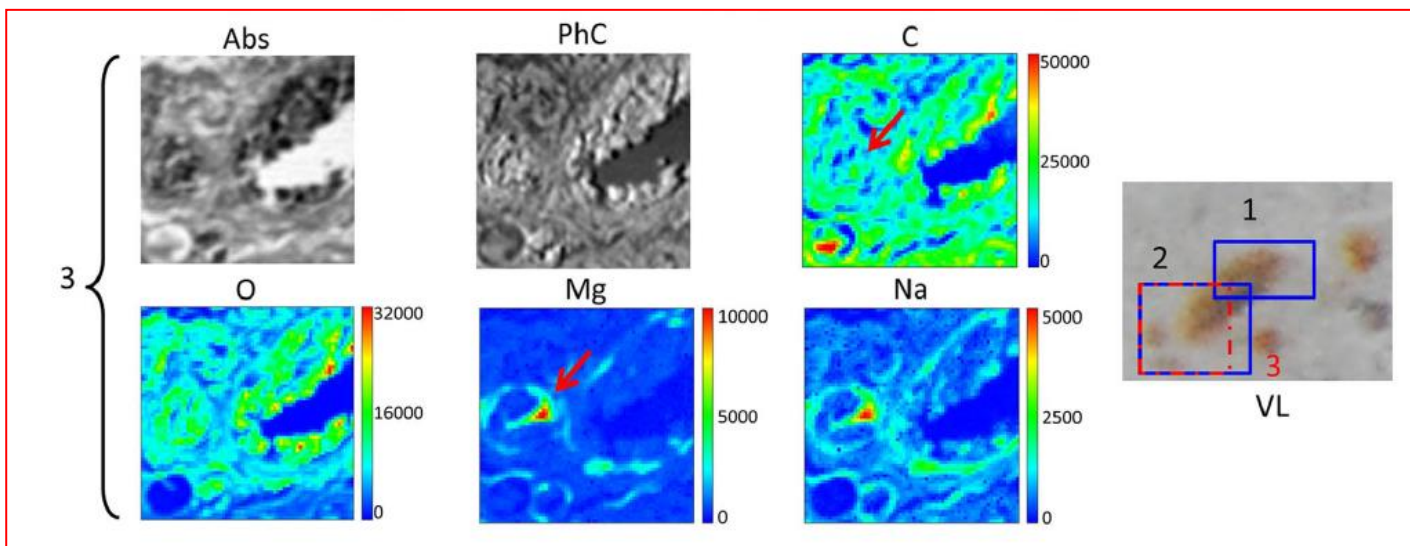
- XRF, with conventional histological analyses, revealed anomalous micro-formations in the pathological tissues and allowed the determination of their elemental composition
- the high Ca concentration is mainly associated with microvessels inside the tissue
- co-localisation of Fe and Zn that mainly corresponds to the presence of red blood cells and capillaries
- the maximal concentration of Fe is related to the presence of blood, while Ca hotspots are located in small areas suggesting microcalcifications.
- in order to better investigate Ca distribution especially in the vasa venorum, high Ca regions were analyzed at lower energy and higher spatial resolution; @7.2 keV setup allows detection of distribution of P and S together with Fe and Ca; 1.5 keV detection of light elements together with Fe

Elemental maps of Ca, P, S and Fe acquired @7.2 keV , 0.5 μm resolution (ESRF France)



Region 2
100 μm x 76 μm
(same as previous)

Elemental maps of Ca, P, S and Fe acquired @1.5 keV , 0.5 μm resolution (Elettra Italy)



Region 3
80 μm x 80 μm

Read the paper for further results on control samples, discussion, developments

Imaging cell morphology and physiology using X-rays

Morphometric measurements, such as quantifying cell shape, characterizing sub-cellular organization, and probing cell-cell interactions, are fundamental in cell biology and clinical medicine.

The main source of morphometric data on cells are the light- and electron microscopies. In the last decades, number of technological advances have propelled **X-ray microscopy** into becoming another source of high-quality morphometric information.

An ideal imaging technique should provide spatial resolution and high penetration power for hydrated specimens, with minimal sample preparation prior to imaging.

Review the status of X-ray microscopy as a quantitative biological imaging modality. Describe the combination of X-ray microscopy data with information from other modalities to generate polychromatic views of biological systems. This combination of data from the same specimen generates a more complete picture of the system than can be obtained by a single microscopy method. Such multimodal combinations greatly enhance our understanding of biology by combining physiological and morphological data to create models that more accurately reflect the complexities of life.

Review – recommended to read

2019, Weinhardt et al doi:10.1042/BST20180036.

Imaging cell morphology and physiology using X-rays

From the cell biology perspective, X-ray microscopes fall into one of two categories, full-field transmission (visualize morphology) and scanning in 2D or 3D (to access physiology information)- In both categories of microscope soft and hard x-rays can be used, depending on the desired penetration depth, spatial resolution and contrast mechanism (see table next slide). While there are multiple examples of using soft x-ray coherent diffraction imaging and hard x-ray microscopy for visualizing cells these techniques are mostly proof-of-principal studies and are not yet allowing the type of systematic studies required in cell biology. The preferred method for morphological studies of single cells is transmission soft x-ray microscopy.

Review – recommended to read

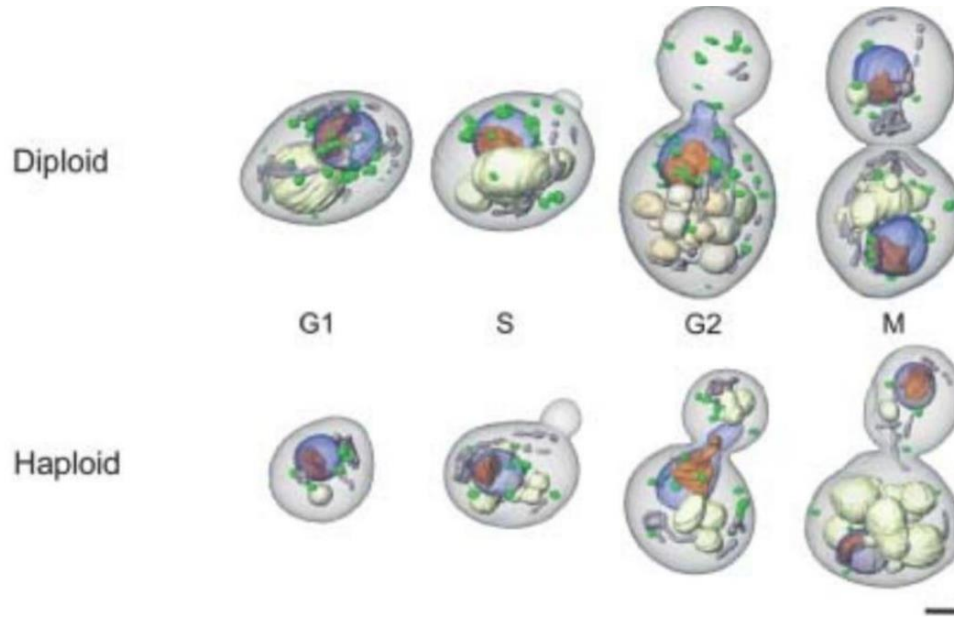
2019, Weinhardt et al doi:10.1042/BST20180036.

List of known and commonly used X-ray microscope methods to study morphology and physiology via trace elements of cells. Contrast, resolution, penetration depth and time required for full acquisition are average values of what has been used in the past for cell biology.

Morphology (transmission)				
Method	Contrast modality	Resolution (nm)	Penetration depth, (µm)	Time required for one tomogram, (mins)
Soft x-ray microscopy (43,58)	“Water window” absorption edges of C, O, & N	25	10	5
Soft x-ray coherent diffraction imaging (40, 42, 52)	Phase-contrast	25	20	50
Hard x-ray microscopy (44–46)	Chemical staining Zernike-like phase contrast	30	60	30
Hard x-ray projection tomography (55–57)	Phase contrast	50	1000	5
Physiology (scanning)				
Soft scanning fluorescence microscope (136,144)	C, N, O, P, & S	25	-	80
Hard scanning fluorescence microscopy (119, 142)	Ca, Fe, Co, & Zn	50	-	180

Investigating the internal morphology of cells

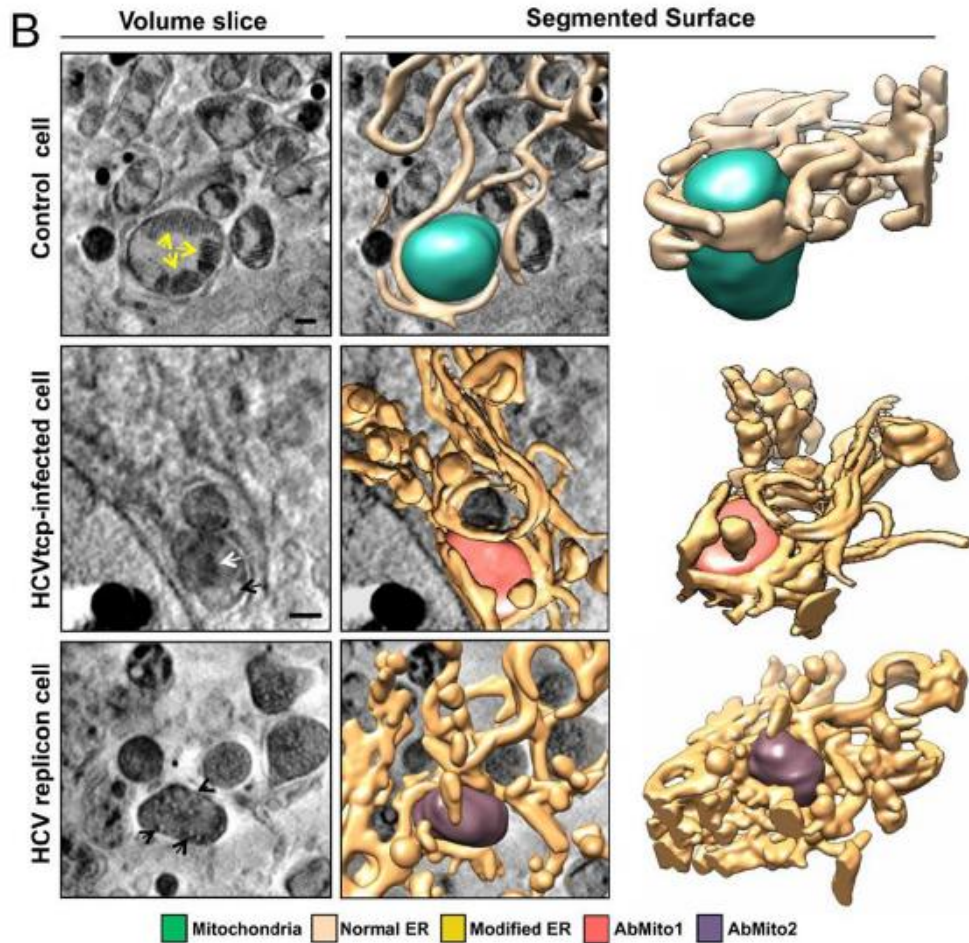
Where electron microscopy would require sectioning of the cells and light microscopy would need the use of multiple fluorescent tags, soft X-ray microscopy provides natural contrast based on X-ray linear attenuation coefficient of all organelles within a cell.



Soft X-ray tomographic study showing the internal morphological changes that takes place during *S. cerevisiae* cell division. Scale bar = 2 μm [77].

Lipid bodies, mitochondria, vacuoles, nucleus, and nucleolus were visualized and measured in 3D at G1, S, G2 and M stages of the yeast cell cycle. Except for vacuoles, the growth of the main classes of organelle was found to be strictly regulated with cell size at all stages of the cell cycle and in both haploid and diploid strains.

Investigating the internal morphology of cells



2019, Weinhardt et al
 doi:10.1042/BST20180036
 Ref [78]

ER structured of affected cell:
 enlarged cisternae, tubular
 structures, vesicular extrusions
 and multiple membrane vesicles

Alteration of the endoplasmic reticulum-mitochondria interface in Hepatitis C virus (HCV) replicating cells [78]. Comparative analysis of the ER-Mito topological relationship of vitrified control (r1), HCVtcp-infected (r2), or HCV replicon-bearing cells (r3). Volumes slices, manually segmented surface representation, and surface views of the different areas of interest are shown. Yellow arrows in (A) mark mitochondrial cristae. Two types of abnormal mitochondria were found class 1 (AbMito1) and class 2 (AbMito2). White and black arrows mark matrix condensation arrows and cristae swelling, respectively. Scale bars 0.5 μm .

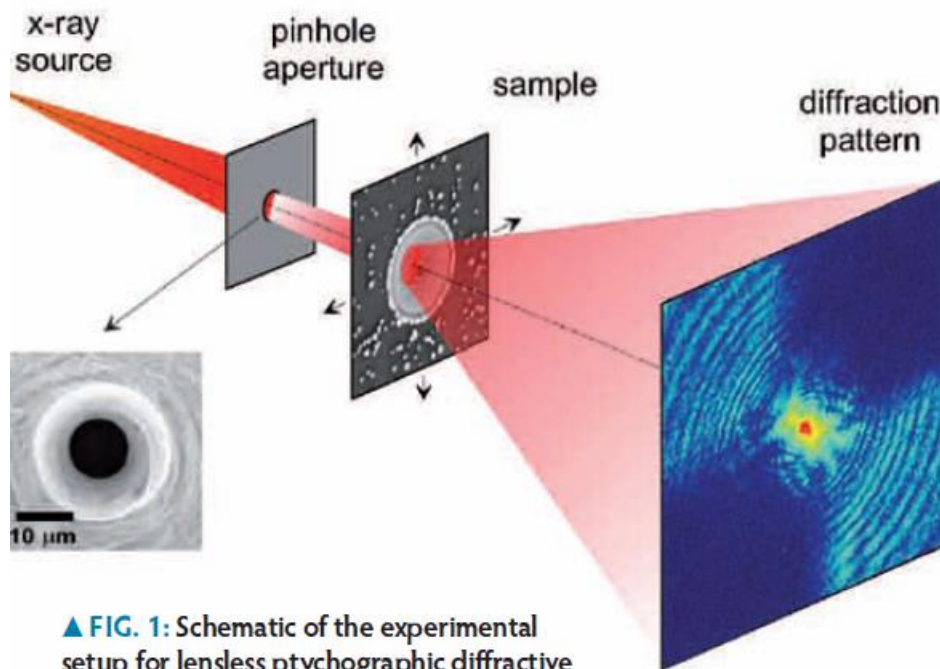
X-ray Coherent imaging

- Coherence of light is generally associated with laser-like properties. Although lasers exhibiting multi-mode oscillations are far from ideal coherent sources, it is true that the wavefronts they produce are highly correlated in space and time.
- This cannot be said about 'classical' sources such as a lamp or a star, which spontaneously emit photons in a chaotic manner, both spatially and temporally. Nonetheless, coherent light can be extracted from a lamp with the help of filtering in the spatial and the temporal domains.
- Spatial filtering is performed by positioning slits or pinholes along the beam path.
- temporal filtering is achieved by extracting a small wavelength bandwidth using a monochromator.
- The price to pay, of course, is a huge loss of intensity. But if the source is sufficiently brilliant to start with, one can afford to pay this price. Third-generation synchrotron radiation facilities are such brilliant sources.

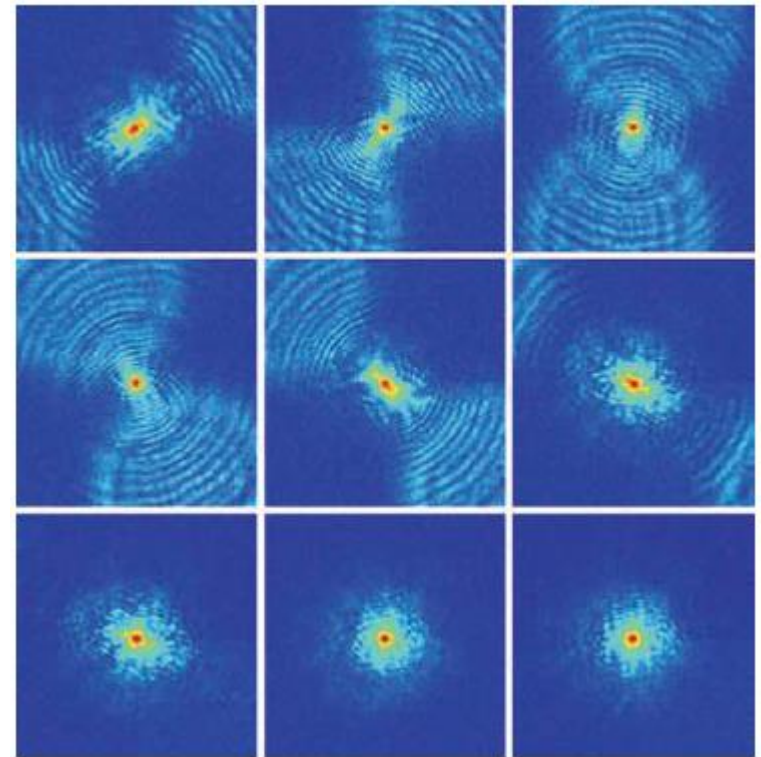
X-ray Coherent imaging

Using standard high brilliance synchrotron and a pinhole aperture a nearly laterally coherent light source can be obtained.

Scanning the samples images at different location can be reconstructed



▲ FIG. 1: Schematic of the experimental setup for lensless ptychographic diffractive imaging. The sample is scanned across the x-ray beam defined by a pinhole aperture and for each sample position a diffraction pattern is recorded by a two-dimensional detector.

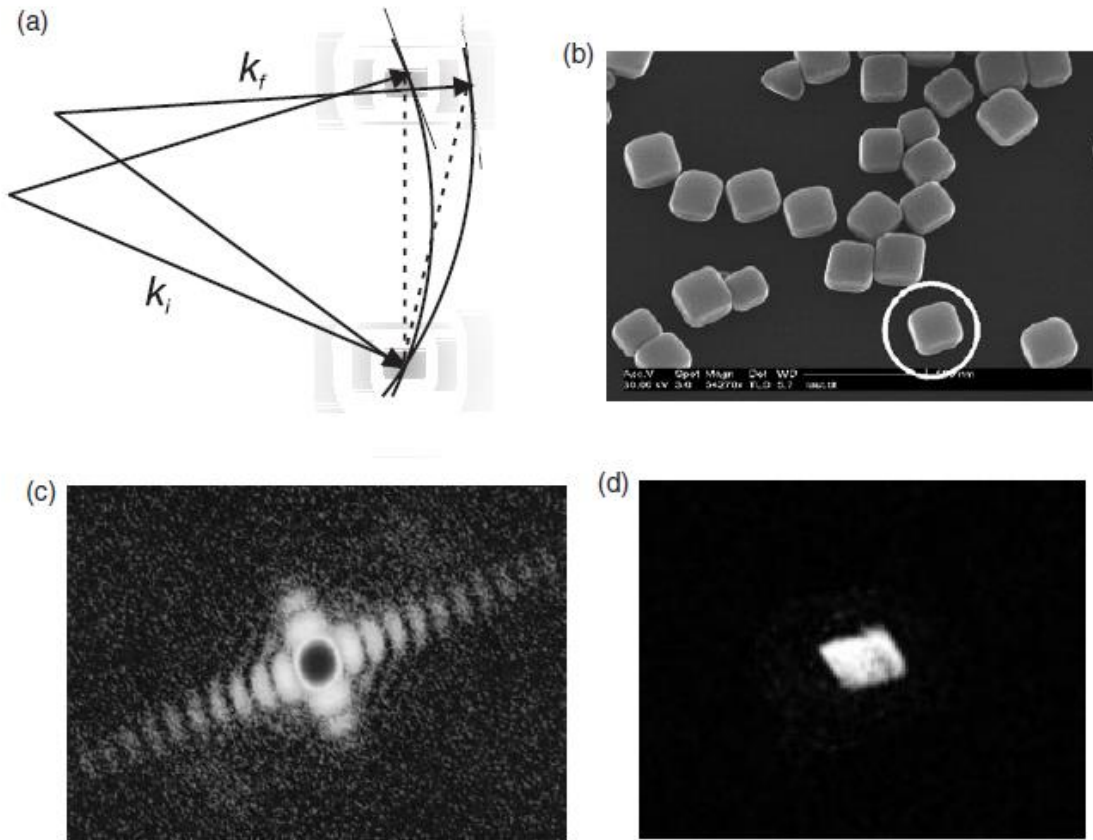


Relation between sample- diffraction pattern - reconstruction

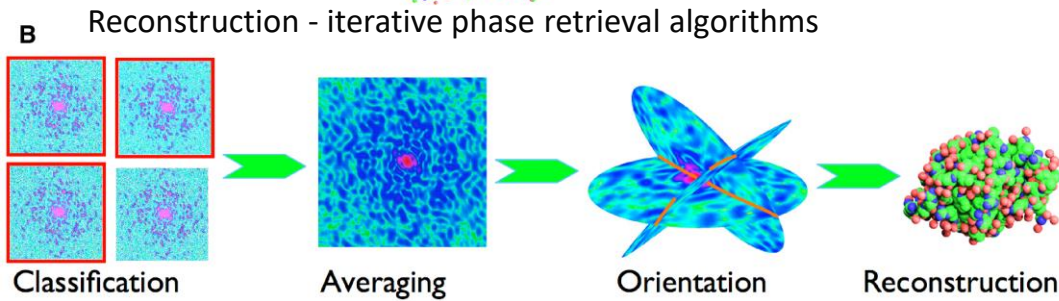
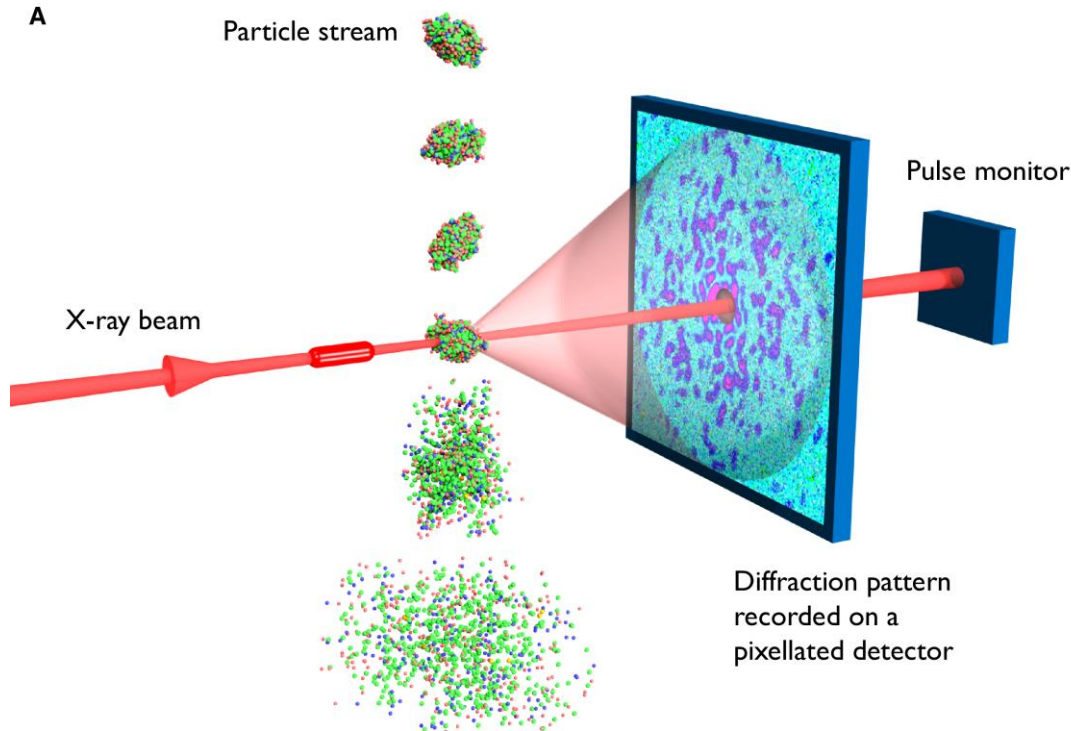
- The diffraction pattern and the light diffracted/scattered by the sample are related by the wave propagation (e.g. Fraunhofer diffraction, which can be modeled by Fourier transforms)
- The diffraction pattern is recorded by the detector as Intensity (Phase is lost)
- The reconstruction of the field at the sample plane is performed by inverse propagation, numerically
- Since the information of the diffraction pattern is Intensity only, the challenge is to find the optimum / realistic reconstruction
- This is done using specific iterative algorithms converging to an optimum solution
- The price to pay, of course, is a huge loss of intensity. But if the source is sufficiently brilliant to start with, one can afford to pay this price. Third-generation synchrotron radiation facilities are such brilliant sources.

X-ray Coherent imaging

Here the structure of a brilliant Bragg peak from a monocrystalline AG cube is used to retrieve the cube shape. Several different angles are used in a tomographic approach



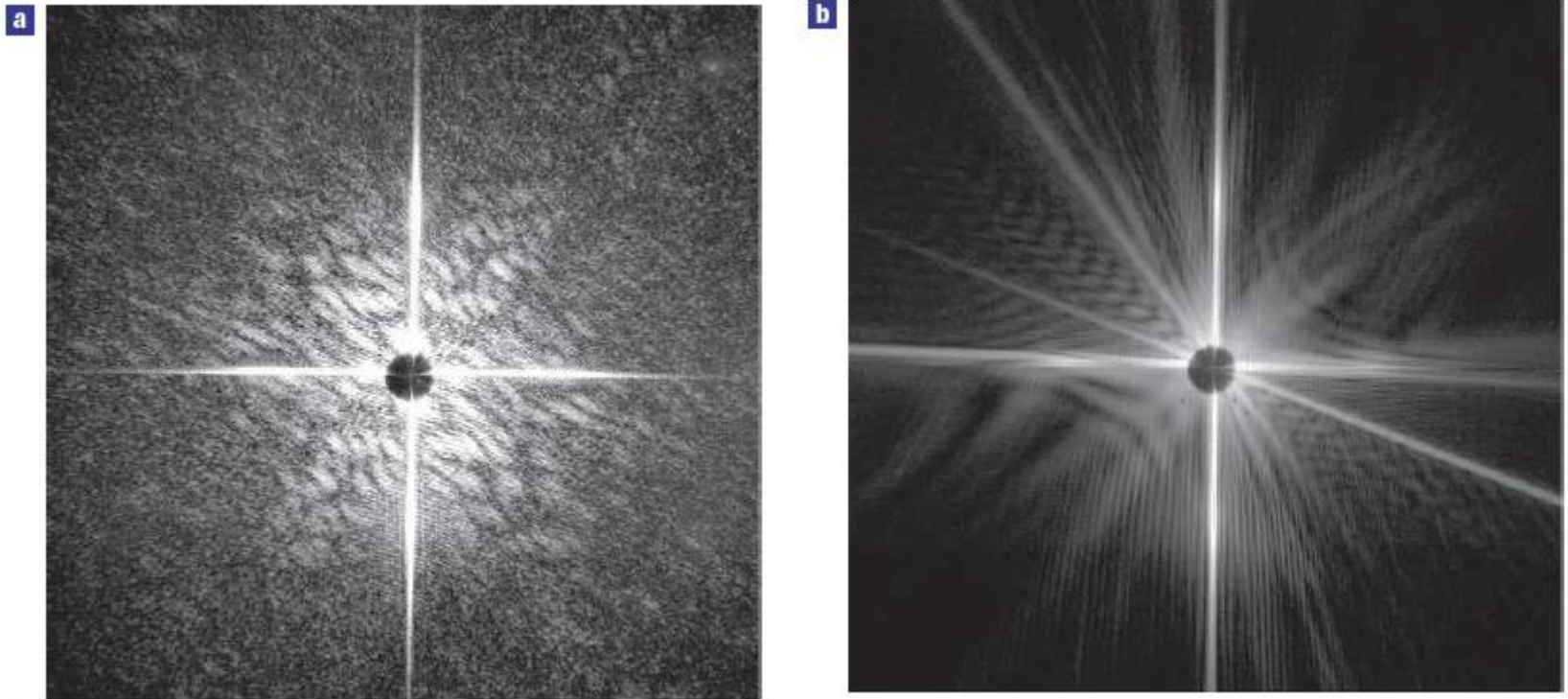
X ray FEL imaging



XFEL single-particle diffractive imaging pipeline involves recording single-shot diffraction patterns of the target object before its destruction due to ionization and Coulomb explosion (top), computational purification of single-particle diffraction patterns, orientation determination, classification into 2D class averages, and the 3D merging of intensities in the reciprocal space.

The Fourier magnitudes are then used to synthesize a real-space image of the object, but only after recovering the phase information that is missing from the diffraction experiment.

YES, damaging is a an issue:



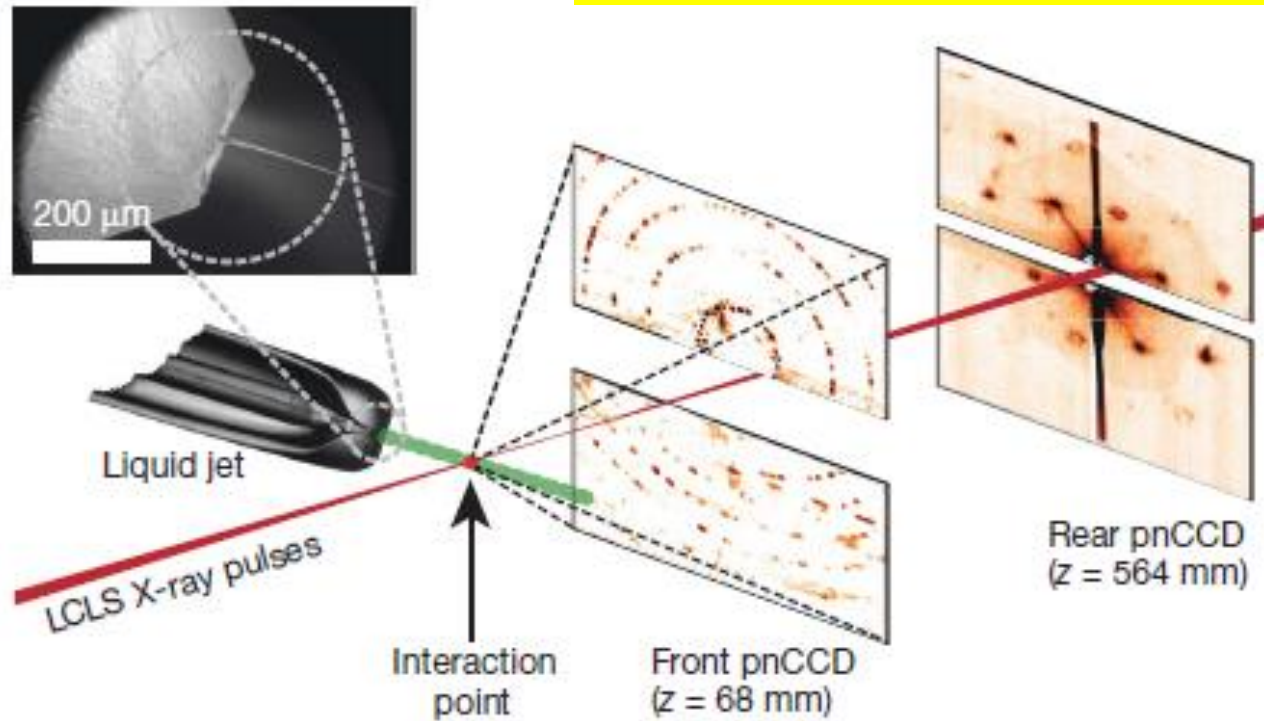
Flash X-ray coherent diffraction patterns. Coherent diffraction patterns recorded for a single $(4\pm 2)\times 10^{14}$ Wcm^{-2} , 25 ± 5 fs pulse (a) and for the subsequent pulse of similar intensity and duration, 20 s later (b), showing diffraction from the damage caused by the pulse that formed (a).

From: E. Chapman et al. Nat Phys., 2006

FEL imaging

BIO-IMAGING

From: E. Chapman et. Al Nature 2011, 2009



- Nanocrystals of Photosystem I (a 1MDa membrane protein complex) flow in their buffer solution in a gas-focused, 4-mm-diameter jet at a velocity of 10m/s perpendicular to the pulsed X-ray FEL beam that is focused on the jet.
- Low and high-angle diffraction from single X-ray FEL pulses are recorded using two CCD placed at different distance from the intaction point. ,
- The FEL repetition rate was 30 Hz.
- Crystals arrive at random times and orientations in the beam, and
- the probability of hitting one is proportional to the crystal concentration.

SUMMARY

- X-ray imaging, contrast mechanisms (intensity attenuation, phase change)
- Other mechanisms due to the interaction of X-ray with matter – fluorescence, Rayleigh scattering, Compton effect
- XrayM schemes: XTM and SXTM and optical components
- X-ray microscopy and spectromicroscopy with Synchrotron light
- Coherent diffraction imaging and FEL imaging
- Examples of application of X-ray microscopy in cell biology

HOMEWORK (for exam)

From the review: 2019, Weinhardt et al doi:10.1042/BST20180036

Choose a relevant biological example, go to the reference paper(s) read and try to explain the imaging scheme, the experiments and the relevance of the work for life science